Preparation and Characterization of Porcelain Electrical Insulator using Sugarcane Bagasse Ash (SCBA)

By: Tamirat Addis Yabiu

A Thesis Submitted to

The Departmentof Applied Chemistry

School of Applied Natural Science

Presented in Partial Fulfillment of the Requirement for the Degree of Master's in Industrial Chemistry

Office of Graduate Studies

Adama Science and Technology University

June 2021

Adama, Ethiopia

Preparation and Characterization of Porcelain Electrical Insulator using Sugarcane Bagasse Ash (SCBA)

By: Tamirat Addis Yabiu

Major advisor: Eshetu Bekele (Ph.D.)

Co-advisor: Eneyew Amare (Ph.D.)

A Thesis Submitted to

The Departmentof Applied Chemistry

School of Applied Natural Science

Presented in Partial Fulfillment of the Requirement for the Degree of Master's in Industrial Chemistry

Office of Graduate Studies

Adama Science and Technology University

June 2021

Adama, Ethiopia

Declaration

I hereby declare that this Master Thesis entitled "Preparation and Characterization of Porcelain Electrical Insulator using Sugarcane Bagasse Ash (SCBA)" is my original work. That is, it has not been submitted for the award of any academic degree, diploma, or certificate in any other university. All sources of materials that are used for this thesis have been duly acknowledged through citation

_____	_____	_____
Name of the Student	Signature	Date

Recommendation

we, the advisors of this thesis, hereby certify that we have read the revised version of the thesis entitled "**Preparation and Characterization of Porcelain Electrical Insulator using Sugarcane Bagasse Ash (SCBA)**" prepared under my/our guidance by **Tamirat Addis Yabiu** submitted in partial fulfillment of the requirements for the degree of Masters of Science in Industrial chemistry.

Therefore, we recommend submitting the revised version of the thesis to the department following the applicable procedures.

Approval of Board of Examiners

The advisors of the thesis entitled "**Preparation and Characterization of Porcelain Electrical Insulator using Sugarcane Bagasse Ash (SCBA)**" and developed by **Tamirat Addis Yabiu**, hereby certify that the recommendation and suggestions made by the board of examiners are appropriately incorporated into the final version of the thesis.

Major Advisor	Signature	Date
Co-advisor	Signature	Date

We, the undersigned, members of the Board of Examiners of the thesis by **Tamirat Addis Yabiu** have read and evaluated the thesis entitled "**Preparation and Characterization of Porcelain Electrical Insulator using Sugarcane Bagasse Ash (SCBA)**" and examined the candidate during open defense. This is, therefore, to certify that the thesis is accepted for partial fulfillment of the requirement of the degree of Master of Science in Industrial Chemistry.

Chairperson	Signature	Date
Internal Examiner	Signature	Date
External Examiner	Signature	Date

Final approval and acceptance of the thesis are contingent upon submission of its final copy to the Office of Postgraduate Studies (OPGS) through the Department Graduate Council (DGC) and School Graduate Committee (SGC).

Department Head	Signature	Date
School Dean	Signature	Date
Office of Postgraduate Studies, Dean	Signature	Date

Acknowledgment

Above all, thanks to Almighty GOD for keeping me in suitable health condition and helping me perform my daily activities without tired and tedious for each of my actions. Next, I would thank Adama Science and Technology University for the best opportunity to achieve a chance to develop my skill and attitude in the profession I do have. It would not have been possible to successfully implement the thesis without the hard work and dedication of the advisor and the support of many other individuals. Thus, I am grateful to my hardworking advisors: Dr. Eshetu Bekele and Dr. Enyew Amare, for their excellent supervision and scientific input in this research work. My special thanks to my mentor, Dr. Eshetu Bekele, whose unique scientific passion and extensive knowledge. I enormously admire and will always aspire to achieve; his patience, daily guidance, and support have kept me on the right track to the end. His positive influence will always be a guide as I venture out on my own to tackle challenging scientific problems. I am lucky to be guided, taught, and advised by him, and in general, his brotherly and humble approach makes me successful. No amount of appreciation can measure my deep gratitude to him and never-ending blessings.

I also wish to express my special gratitude for my friend Abraham Abdo, Tigist Abebe, and Hiwot Bezuneh. They are at my back from the beginning of my M.Sc. study in financial, psychological, and moral support advice during my research work until the final success.

My sincere gratitude also goes to Adama Science and Technology University for their sponsorship of this research work. I want to thank technicians' (especially Guta Amenu from chemistry, Bundi Roba from chemical engineering, Shumi from geotechnical engineering). Thank you very much for being there, contributions to the laboratory apparatus, for their open-minded help during laboratory work and data analysis.

I want to express my gratitude to Dr. Tatek Dejene and Dr. Dereje Tsegaye for their support, guidance, and valuable criticisms of the statistical interpretation. I wish especially to thank Dr. Belay Brhane for his helpful comment and approval.

Finally, and humbly, I wish to extend my warm thanks to all the good people in the Geological Survey of Ethiopia, in the Ethiopian assessment conformity enterprise, and Addis Ababa University for their contribution to this work.

Table of Content

Content **Page**

List of Figures

List of Tables

Acronyms and Abbreviations

AAS ..... Atomic Absorption spectrometer

AF ..... Arerti feldspar

ASTM. ..... American Standard for Testing Materials

BC.....Bombowua clay

CS ..... Chancho sand

DC.....Denkaka clay

DTA. ..... Differential Thermal Analysis

ICDD ..... International Center for Diffraction Data

LL ..... Liquid Limit

LOI .....Loss on ignition

MOR ..... Modulus of rupture

PI.....Plastic Index

PL .....Plastic Limit

SCBA .....Sugarcane bagasse ash

SEM. ..... Scanning Electron Microscopy

TA.....Thermal Analysis

TGA. ..... Thermogravimetry Analysis

WF ..... Wolkite Feldspar

XRD.....X-ray Diffraction

a.u. ..... Arbitrary unit

Abstract

In this study, two clay materials mined from Bombawuha (BC) and Denkaka (DC), two feldspar materials collected from Arerti (AF) and wolkite (WF) and quartz mined from Chancho (CS), as well as SCBA waste collected from Wonji Shewa sugar factory of Ethiopia was characterized to evaluate their potentials as raw materials for producing quality electrical porcelain insulators. A total of 5kg samples of the aforementioned raw materials were collected, dried, and ground to sieve size of 63µm for clays, feldspars, and sugarcane bagasse ash and 45µm for sand, then the mineralogy, chemical composition, thermal property, plasticity, and particle size distribution of raw materials were characterized by using x-ray diffractometry (XRD), atomic absorption spectrometer (AAS), Thermogravimetry analysis (DTA-TG), Atterberg plasticity test, sieve-hydrometer analysis, respectively. Four different body compositions were formulated by varying the relative proportion based on the raw material potential characteristic. A total of one hundred thirty-two (132) (one hundred eight (108) a cylindrical shaped for physical and electrical strength test and twenty-four (24) a rectangular-shaped for mechanical strength test) bodies of the desired formulations were prepared and labeled as with composition SCBA0 (50% clay, 40% mixed Feldspar, 10% sand and 0% SCBA), SCBA10 (50% clay, 30% mixed Feldspar, 10% sand and 10% SCBA), SCBA15 (50% clay, 25% mixed feldspar, 10% sand and 15% SCBA) and SCBA20 (50% clay, 20% mixed feldspar, 10% sand and 20% SCBA), the batches were fired at firing temperature of 1200°C, 1250°C, and 1300°C and firing time of 1.5hr, 2hr and 2.5hr. Finally, the fired products were investigated for their physical properties (water absorbance, bulk density, and apparent porosity), electrical properties (dielectric strength), mechanical strength (modulus of rupture), and phase analysis by XRD. The physical-mechanical properties and dielectric strength measured for each porcelain sample confirmed batch SCBA10 with the composition of (10% SCBA waste, 50% BC, 30% mixed Feldspar (AF and WF in 50:50%), and 10% CS) fired at 1250°C and at firing time 2.5hr was found to have the dielectric strength of 6.59 kV/mm, bending strength of 42.53 MPa and water absorption of 0.35%, which satisfies the obligatory properties for porcelain insulators. In conclusion, this study confirmed that quality porcelain electrical insulators could be produced using locally available raw materials (Clay, Feldspar, and quartz) and the partial replacement of Feldspar by sugarcane bagasse ash waste.

1. INTRODUCTION

1.1 Background of the Study

Developments of the modern world depend significantly upon a continuous electric power supply. But, with growing demand, utilities must provide secure and reliable power delivery while maximizing the performance of the power distribution system from both technical and economic standpoints. Interruptions or failures within the power systems may damage valuable high-voltage equipment and lead to considerable loss of revenue, mainly for industrial consumers. For this reason, an insulator is used in the transmutation and distribution system of electric power to deliver the electric energy to the intended customer safely.

Insulators are among the critical devices of electric power transmission systems. The efficiency of transmission and distribution of electric power depends, among other factors, on the quality of electric insulators since it has to prevent unwanted flow of electric current to the earth from its supporting points. Insulators are to be attached to the tower, and at the same time, they are electrically insulated from the grounded towers. They are essentially required for two primary purposes: i) to isolate the transmission tower from the high-voltage source, and ii) to provide a load-bearing platform capable of supporting heavy overhead conductors well above the ground (Looms & Chapman, 1991). Hence insulators need to withstand stable voltages and over voltages, such as lightning, and various environmental stresses such as rain, snow, and pollution.

An insulator ideally is a substance that does not allow an electric charge to flow through it and does not affect the electric fields (Cherney et al., 2014). They are made from dielectric materials with high electric resistance and dielectric constants such as glass, porcelain, and composite materials. Porcelain materials are among the primary materials used for insulation on power transmission and distribution lines (Nasejje & Sam, 2015). Each of the three dielectric material (i.e porcelain, glass and composite) has a number of advantage and disadvantage, but porcelain insulator is widely used as insulators in electrical power transmission systems due to the raw materials are readily available at lower cost compare to other types of insulators which are based on industrially processed materials and they are resistant to high temperature, electricity, and harsh environment than polymers (Moyo & Park, 2014) ; they are superior electrical properties, absence of creep or deformation under stress at room temperature and more excellent resistance to

environmental changes; they are not sensitive to the minor differences in composition, fabrication, techniques, and firing temperature (Demchuk et al., 2009; Islam et al., 2004); they have a very long lifetime ranging from 10 to 20 years even some are over 70 years or more and consist of all the significant characteristics of ceramics such as; insulating capabilities, dimensional stability, hardness, thermal resistance, and resistance to corrosion. These are reasons for their wide range of applications in the safe transmission of electricity (Onwughalu & Ogwata, 2019) and their continued use over the decades, despite the emergence of new insulator materials like plastics and composites (P. W. Olupot et al., 2010).

Clay, Feldspar, and quartz are the potential raw materials for the production of porcelain insulators. Each of these raw materials plays a specific role in influencing the properties and performance of the final products (P. Olupot, 2006). Clay provides the plasticity and is a source of alumina, which, together with quartz and alkaline fluxing elements, forms mullite and glassy phase during the firing process. Both phases contribute to the improvement of the mechanical and dielectric strength of a porcelain insulator. Feldspar promotes vitrification and densification of the porcelain sample at the end of the firing process. Quartz maintains a porcelain structure and regulates the ratio between SiO_2 and Al_2O_3 to form mullite ($3Al_2O_3 \cdot 2SiO_2$). Therefore, the composition of the raw materials influences the physical-chemical properties of the resulting ceramics due to series of transformation which occur upon firing within the sintered body (Bergmann, 2004). The effect of variations in the composition of the raw materials in the properties of porcelain insulators depends on the method of production, the firing temperature adopted and firing time (P. Olupot, 2006).

Today, the whole world is suffering from two types of problems, i.e., the disappearance of virgin resources (material and energy) and excess production of waste material. From the perspectives of the economies, material and energy needs, and environments of developing and developed nations, the only way to eliminate these problems is to utilize economic materials such as waste in the main production streams. Following this realization, the ceramics industry is also seeking to use waste as a resource in its productions. Additionally, to improve production, ceramic manufacturing requires reducing production costs, especially energy costs. This may be achieved by adopting fast firing cycles and using fluxes (Njoya et al., 2017).

Many researchers concentrated efforts to find a flux material with technical and economic feasibility to use porcelain electrical insulators. Flux material plays an essential role in the final microstructure of ceramic products. During firing, these materials form a liquid phase that fills the pores, decreasing porosity and water absorption, promoting the thermodynamic conditions for the growth of mullite crystals and increasing mechanical strength. However, to encourage the desired effects, the liquid formed during burning must have an adequate amount and viscosity characteristics (William Ochen, Florence Mutonyi D'ujanga, 2019).

Feldspar is the flux material most widely used by porcelain manufacturers since it is responsible for obtaining products with excellent technical and aesthetic properties. The resources of high-grade feldspar minerals have recently begun to become depleted. The high price cost raw material compared to the other two raw materials (i.e., Clay and quartz). Thus, it is necessary to evolve an alternative source of abundantly available fluxing materials for porcelain bodies, lowering the temperature's viscous liquid forms (Kausik Dana & Das, 2004b). As a result, some waste has been identified as a potential source of Feldspar, e.g., soda-lime glasses (Matteucci et al., 2002), blast furnace slag (Kausik Dana & Das, 2004b), metallurgical slags (K. Dana & Das, 2003), rice straw ash (RSA), rice husk ash(RHA) (Prasad et al., 2001), silica fume (SF) (Prasad et al., 2002), fly ash (FA) (Kausik Dana & Das, 2004a). However, secondary raw materials are considered feasible if sufficient and reliable amounts and quality materials are available, and the product quality and properties are not impaired.

The last few decades have seen a rapid growth of sugar industries in Ethiopia, accounting for a significant percentage of gross national products. At the same time, these industries have added vast quantities of solid wastes and secondary materials to our environment. One of the solid wastes is sugar cane bagasse ash (SCBA). Therefore, these materials are usually dumped on open grounds or buried in landfills, and the impacts of which on the environment have been disastrous. The optimistic solution to the disposal problem of the SCBA is to decrease the quantity of disposal with the utilization of waste in the industry. The valorization of industrial wastes and their up-grading to alternative raw materials can present several advantages when compared with the use of primary natural resources, namely reduction in the extraction volume of natural raw materials (resource preservation), lower energy consumption during subsequent processing (reduced costs), and lower pollutant emission levels (improvement of population health and safety). Even if the

waste incorporation is done in small amounts, high production rates will translate into significant consumption of waste materials. Moreover, waste materials might constitute a cheap renewable raw material source for the industry to use (Junkes et al., 2012).

Thus, SCBA waste is similar in chemical composition to common natural aluminosilicate porcelain raw material (Feldspar for this study) used to produce porcelain insulators. This means that the reuse of SCBA waste as a possible alternative source of Feldspar for porcelain insulator production is an essential technological solution. Hence, it is thought that using this waste in the production of porcelain insulators will be the remedy for environmental problems. It might also improve the quality of the insulator and lower the firing temperature leading to cost cuts (Viruthagiri et al., 2015).

Previously, the Ethiopian electric power corporation utilized locally manufactured and imported insulator material, but the locally manufacture porcelain insulator primarily relied on imported goods such as scarcely available foreign raw material (ball clay) imported from England. The local manufacturer (Tabor ceramic industry) stopped manufacturing porcelain insulators mainly due to a lack of reliable locally available quality ceramic raw material. Such a state of affairs adversely affects the country's foreign exchange reserve and is inconsistent with the driving force for local substitution of imported goods. Moreover, it is an obstacle to the big dream of the country's short and long-term rapid-developing strategy. Therefore, investigating the local potential of raw materials to develop quality overhead insulators from locally available and economically recyclable raw materials needs prior attention to extend the country's sustainable development.

Therefore, this study aims to develop electrical porcelain insulators from locally available raw material and waste materials by optimizing batch composition, firing temperature, and firing time of the production process.

1.2 Statement of the Problems

In Ethiopia, despite the enormous availability of natural raw materials and recyclable materials, the production of quality porcelain insulators couldn't be succeeded. For instance, Clay found in Bombowha and kombucha zone of Oromia regional (Fentaw & Mengistu, 1998), as well as the Clay found in Belesa (hosanna) and Ansho area of the southern region of Ethiopia (Fentaw & Mengistu, 1998; Merga et al., 2019), have shown a characteristic potential property required for porcelain insulator fabrication when compared to clays utilized for porcelain production in literature (Moyo & Park, 2014; P. W. Olupot et al., 2010; Yaya et al., 2017). Moreover, potential deposits of Feldspar and quartz were also found in Arero woreda, Guji zone of the Oromia region, etc. (Merga et al., 2019).

During the preliminary study, the only manufacturer of porcelain insulator in Ethiopia, the tabor ceramic industry has stopped manufacturing due to a lack of proper scientific investigations on the characteristics of available porcelain raw materials and technical problems that occurred associated with formulation; manufacturing process, and other reasons that results in low quality and high cost of manufacturing porcelain insulator. On another side, the growing demand for high voltage porcelain insulators in Ethiopia is potentially enormous for power transmission and distribution. Consequently, to meet the request, the country expends much in foreign exchange in importing high voltage porcelain insulators from abroad. Such a state of affairs adversely affects the country's foreign exchange reserve. It is inconsistent with the country's short- and long-term development strategy, which considered import substitution one of the strategic issues that need to be addressed.

The grade of porcelain raw materials (Clay, Feldspar, and quartz) is essential for producing quality and low-cost porcelain insulators. In this regard, the quality of Feldspar, which is added to decrease firing temperature and thus to reduce cost by saving fuel (energy) and allowing a virtually zero (<0.5%) open porosity and a low level of closed porosity (<10%) has the significant role in the production of low cost and high-quality porcelain insulator. The grade of Feldspar mainly depends on the alkaline oxide ($K_2O + Na_2O$) content. The previous study (Merga et al., 2019) in Ethiopia indicates that Aero feldspar that Tabor Ceramic has used has low flux or alkaline oxide content ($K_2O + Na_2O < 5$ wt.%) compared to the chemical composition requirement of Feldspar in porcelain production ($K_2O + Na_2O > 12$ wt.%). The reported amount of alkaline or flux in Arero Feldspar may lead to either rising energy consumption or extensive usage of Feldspar to get

sufficient glassy phase in porcelain body. Still, such practices are not appropriate due to the comprehensive exploration of natural resources and increased product cost due to high energy consumption. However, this study aimed to overcome such problems by partial substitution of Feldspar by recyclable materials like sugarcane bagasse ash waste that contains high silica and a sufficient amount of flux or alkaline oxide to yield the required glassy phase at a relatively lower temperature. Moreover, recycling waste materials contributes to the fulfillment of the Ethiopian green economic strategy by minimizing the environmental burden associated with the existing waste management practice and extensive usage of natural resources.

1.3 Objectives

1.3.1 General Objective

The general objective of this study is to investigate the potential of sugarcane bagasse ash to produce high-quality and lower-cost porcelain electrical insulators by partial replacement of ceramic raw material (Feldspar).

1.3.2 Specific Objectives

To characterize the raw material (clay, feldspar, and quartz) and waste material (SCBA) to mineralogy, chemical composition, thermal properties, particle size distribution, and plasticity.

To produce electrical porcelain insulator by partially replacing low alkaline feldspar with locally available sugarcane bagasse ash waste by Optimizing batch composition, firing condition, and firing time.

To Characterize produced porcelain insulators concerning physical properties (i.e., porosity, water absorbance, and density), electrical properties (dielectric strength), mechanical strength (flexural strength), and phase analysis of the materials.

1.4 Significance of the Study

The raw materials and waste material characterization results of the studied materials help document the potential of indigenous ceramic raw materials and waste material used as reliable secondary data sources for any activity regarding the materials and promote the country's natural resource proper utilization trends. This study also encourages and attracts local microenterprises and investors to participate in new ceramic industry expansions; thus, it creates new job opportunities for citizens in mining materials, transportation, production, and selling. Moreover, incorporating sugarcane bagasse ash wastes in porcelain electrical insulators provides a way of converting these wastes into valued products, which reduces environmental problems by avoiding landfill disposal and water pollution. In addition to this, the SCBA waste can also save natural feldspar raw material by partially replacing it.

2. LITERATURE REVIEW

2.1 Overview of Electrical Insulator

In recent years, electricity has become one of the most necessities of inhuman life. Extra high voltage power lines have been widely used to transmit the electric energy from the power stations to the end-users. From the perspective of consumption electricity, it has been significantly increasing in developing countries due to increased population and level of industrialization. For instance, in Ethiopia, the energy sector has been growing in the past two decades and reached a currently electric power of 2360 MW; this would be expected to reach 10,000 MW in the next ten years (Mondal et al., 2018). Overhead transmission lines are responsible for delivering electric power from generators to industrial and residential customers. The energized conductors on the overhead transmission lines must be attached to the tower while electrically insulated from the grounded towers. The device that can hold the weight of the conductors while it provides electrical insulation between the line and the tower is called an insulator.

Insulators are among the critical devices of electric power transmission systems. They play a significant role in maintaining the reliability of the network. They are materials that inhibit the current flowing in electrical circuits (Islam et al., 2004). The need for electrical insulators is essentially to prevent the passage of electricity to some other device or area so that the electricity does not cause harm or cause death to those who touch areas or devices which are connected to the electrical insulators (Ezenwabude & Madueme, 2015; Moyo & Park, 2014). They must be electrically inert and isolate two conductors of different potentials (Cajetan et al., 2015). Most insulators have outdoor applications subjected to environmental conditions such as moisture, high temperature, contamination, and icing. To choose the right type of insulator before the installation, the site's environmental conditions must be studied.

Nowadays, insulators adopted for transmission/distribution are made of ceramic, glass, or polymeric type. Porcelain and glass insulators have been used for a long time, and there is considerable experience in manufacturing, installation, and their field performance is well known. Composite insulator represents the last acquisition in the field of outdoor insulation; their use began recently and knew an explosive development in the previous years (Moyo & Park, 2014).

2.2 Porcelain Electrical Insulator

Porcelains are vitrified ceramic white wares used widely in the household, laboratory, and industrial applications (P. Olupot, 2006). The porcelain body is achieved by heating Clay raw materials in the furnace between 1200 to 1400°C. The porcelain toughness, strength, and translucence are due to the development of glass and the mullite phase within the fired porcelain body (Oladiji et al., 2010). Porcelain was veritable stoneware due to its high density, industrial fast firing cycles, real mechanical strength, and wear resistance (Onwughalu & Ogwata, 2019).

Porcelain electrical insulators are generally ceramic materials made by heating raw materials (Clay, Feldspar, and quartz) in a kiln to a temperature between 1,200 °C and 1,400 °C, and they prevent the flow of electrical current through them (Cajetan et al., 2015). Porcelains are widely used as insulators in electrical power transmission systems due to the high stability of their electrical, mechanical, and thermal properties in the presence of harsh environments. These are the reasons for their continued use over the centuries despite the emergence of new materials like plastics and composites (Cajetan et al., 2015).

For the electrical insulation application, the most required properties of the porcelain electrical insulator are high mechanical strength and high dielectric strength to withstand high voltage. However, high mechanical resistance, low prosperity, and water absorption are among other essential properties of electrical porcelain. A specific composition of raw materials may achieve the increased strength of electrical porcelain. Still, due to geological and geophysical characteristics, the raw materials may have various chemical compositions and specifications (Ngayakamo & Eugene Park, 2019).

2.2.1 Porcelain Insulator Raw Materials

The primary raw materials for porcelain insulators are Clay (kaolin), Feldspar, and quartz, all characterized by small particle sizes (Jamo, 2015). The properties of the different Clay ceramic products are critically influenced by the relative concentrations of the three main components in their pastes: Clay (kaolin), quartz, and Feldspar. The Clay gives plasticity to the ceramic mixtures. At the same time, flint or quartz maintains the shape of the formed article during firing, and Feldspar serves as flux, which is added to decrease firing temperature and thus reduce cost by saving fuel (energy) (Ovri & Onuoha, 2015)

2.2.1.1 Clay

2.2.1.1.1 Definition Clay and Clay Minerals

The term "clay" refers to a naturally occurring material composed primarily of fine-grained minerals, which are generally plastic at appropriate water contents and will harden when dried or fired. Clay usually contains phyllosilicates; it may contain other materials that impart plasticity and harden when dried or fired. Associated phases in Clay may include materials that do not impart plasticity and organic matter. It also denotes the finest fraction of sediment or soil in the classification of Clay, silt, and sand. The particles of most clay minerals are tiny, and it is only rarely that their 'equivalent' size exceeds 2 µm (Guggenheim et al., 1995).

The term "clay mineral" refers to phyllosilicate minerals and minerals that impart plasticity to Clay and harden upon drying or firing. Clay minerals are layer silicates usually formed as chemical weathering of other silicate minerals at the earth's surface (Guggenheim et al., 1995). Generally, Clay is a natural, earthy, and fine-grained material comprised of a group of crystalline minerals known as clay minerals.

2.2.1.1.2 Classification and Properties of Clay Minerals

Clay minerals are predominantly silicates of aluminum and/or iron and magnesium. Some of them also contain alkalies and/or alkaline earth as essential components. These minerals are mostly crystalline, so that the atoms composing them are arranged in definite geometric patterns. Most of the clay minerals have sheet or layered structures. The sheet silicates consist of "composite layer" sheets of tetrahedrally coordinated Si, Al, and octahedrally coordinated cations (mainly: Fe^{3+}, Fe^{2+}, Al^{3+}, and Mg^{2+}) (Mejia, 2013).

According to the sheet type, silicate clay minerals can be classified as clays of two-layer or 1:1 type represented by the kaolin and serpentine. As clays of three-layer or 2:1 type described by the illite-mica, smectite, vermiculite, and chlorite groups (Murray, 2000). The corresponding classification of clay minerals is listed in Table 2.1.

Table 2.1: Classification of clay minerals according to the sheet type silicate.

Layer type	Group	Mineral species
1:1	Kaolin	Kaolinite, Dickite, Nacrite, Halloysite
2:1	Illite-Mica	Illites, Muscovite, glauconite, celadonite, paragonite.
	Smectites	Montmorillonite, Beidellite, Nontronite
	Chlorite	Clinochlore, chamosite, pennantite, etc.
	Vermiculite	Vermiculite

As shown in table 2.1, Kaolin is formed by two layers that comprise one tetrahedral and one octahedral sheet in the unit cell. Illite- mica, smectite, vermiculite, and chlorite consist of three layers built up by one octahedral sheet sandwiched by two tetrahedral sheets in the unit cell.

Generally, the utility of a clay mineral in specific applications are due to their physical and chemical properties, which are mainly dependent on two factors: (a) their crystal structure, which can be either a 1:1 structure (one tetrahedral sheet bound to another octahedral sheet) or a 2:1 structure (one octahedral sheet between two tetrahedral sheet) and (b) their chemical composition. Additional factors are essential in determining a clay's properties and applications: the non-clay mineral composition, organic material content, the type and amount of exchangeable ions and soluble salts, and the texture (Moraes et al., 2017).

A. Kaolin Minerals

The kaolin group minerals comprise kaolinite, nacrite, dickite, and halloysite, and are among the most common clay minerals in nature. They have a 1:1 layered structure; each layer consists of one tetrahedral silicate sheet and one octahedral sheet, with two-thirds of the octahedral sites occupied by aluminium, as shown in the figure 2.1 (Ngoc, 2012). The two sheets are held together in such a way to form a single layer with 7.2 ˚A in thickness and extend indefinitely in the other two directions. The successive layers of the primary layer are stacked together by hydrogen bonds between the hydroxyls of the octahedral sheet and the tetrahedral sheet's oxygens. Because the Kaolin sheets are held together by hydrogen bonds that prevent expansions which also contains an entry of polar molecules hence a low cation exchange capacity (CEC) of 10 to 100 mmolkg^{1}

(Murray, 2007). Kaolinite, nacrite, and dickite all have the ideal chemical composition: $Al_2Si_20_5(OH)_4$; they differ only in how the 1:1 layers are stacked. Halloysite, in its fully hydrated form, has the ideal chemical formula $Al_2Si_20_5(OH)_4.2H_2O$. Kaolinite differs from the other three group members by including molecular water in the interlayer (Murray, 2007). Moreover, the cation exchange capacity (CEC) of kaolinite is less than that of montmorillonite due to its low surface area and low isomorphous substitution resulting from its high molecular stability contributes to its low plasticity, cohesion, shrinkage, and swelling (Ochieng, 2016). The structure of the Kaolinite mineral is presented in Figure 2.1 (Murthy, 2005).

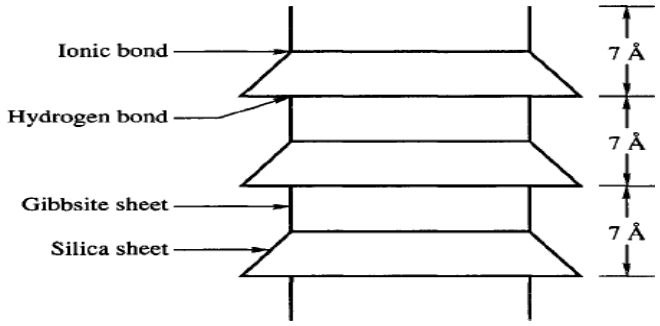

Figure 2.1: Structure of Kaolinite layer

B. Smectite/montmorillonite Minerals

Smectite, which includes montmorillonite, beidellite, nontronite, saponite, and hectorite minerals, comprises two silica tetrahedral sheets with a central octahedral sheet designated as a 2:1-layer mineral (Figure 2.2). The layers are stacked together by van der Waals bonds rather than a week compared to hydrogen bonds, and there is a net negatively charge deficiency in the octahedral sheet. Water and exchangeable ions can occupy and separate the layers (Murray, 2007).

Smectites have skinny layers and small particle sizes, contributing to high surface area and a high degree of absorbency of many materials such as oil, water, and other chemicals (Zbik et al., 2010). Additionally, smectites have higher cation exchange capacities, swelling, and shrinkage properties than other clays. The variable net negative charge on smectite's structural layers attracts water molecules into the interlayer area, causing expansion. The amount of swelling is related to the type of interlayer cation present. Generally, Soils dominated by these types of minerals form a wide range of cracks upon drying up, and the resultant dry aggregates are very hard hence making the

soil challenging to till (El-Maarry et al., 2013). The structure of the mineral is presented in Figure 2.2 (Murthy, 2005).

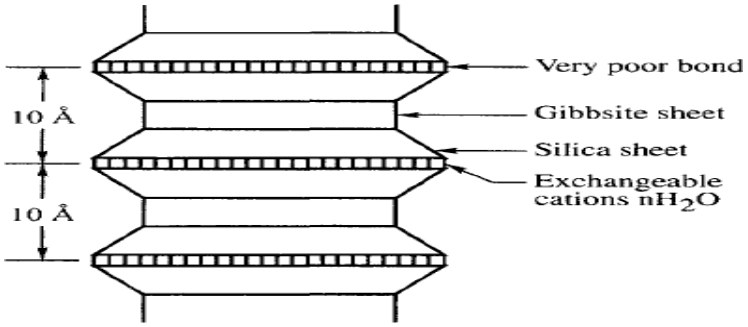

Figure 2.2: Structure of Montmorillonite layer

C. Illite

Illite is a general term for clay constituents or argillaceous sediments that belong to the hydrous mica group. It is a significant rock-forming mineral being a central component of shales and other argillaceous rocks with a formula, $(K, H)Al_2(Si, Al)_4O_{10}(OH)_2.xH_2O$, where x represents the variable amount of water that exists in illites (Murray, 2007). It has a basic structure consisting of a sheet of alumina octahedrons between and combined with two sheets of silica tetrahedrons. This clay mineral has a structure similar to montmorillonite, but the layers are more strongly bonded together. The layers are separated by potassium ion in illite, whereas in montmorillonite, the layers are separated by loosely held water and exchangeable metallic ions (Figure 2.3). The bonds with the non-exchangeable K^+ ions are weaker than the hydrogen bonds but stronger than the water bond of montmorillonite. Unlike montmorillonite particles, which are extremely small and have a great affinity for water, the illite particles will normally aggregate and develop less affinity for water than montmorillonites (Cernica, 1995). The structure of the mineral is presented in Figure 2.3 (Murthy, 2005).

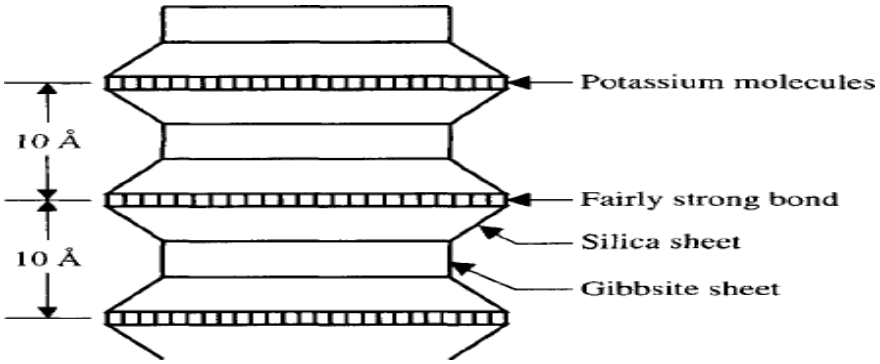

Figure 2.3: Structure of Illite layer

D. Chlorite

Chlorite is made of repeating layers of silica sheet, an aluminum sheet, another silica, and either a gibbsite (Al) or brucite (Mg) sheet (figure 2.4). It could be called a 2:1:1 mineral. Chlorite can also have many isomorphous substitutions and be missing an occasional brucite or gibbsite layer; thus, it may be susceptible to swelling because water can enter between the sheets. Generally, however, it is significantly less active than montmorillonite (Holtz et al., 2013). The composition of chlorite is usually shown as $(OH)_4(SiAl)_8$ (Mg- Fe)$_6O_{20}$. The brucite-like sheet in the interlayer position has the general composition $(MgAl)_6(OH)_{12}$ (Reeves et al., 2006). The schematic diagram of chlorite is presented in figure 2.4 (Holtz et al., 2013).

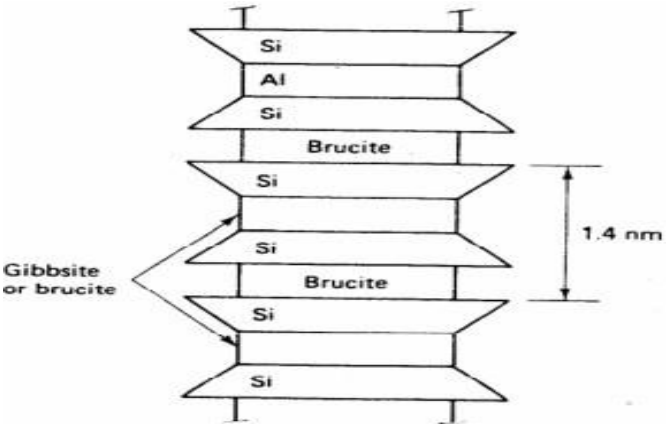

Figure 2.4: schematic diagram of chlorite

E. Vermiculite

Vermiculites are similar in structure to the smectites (Figure. 2.5) but have a more significant net negative charge on the composite layer of 0.6-0.8 per $O_{10}(OH)_2$. The principal interlayer cations

are hydrated magnesium. Vermiculites exhibit swelling properties similar to the smectites but to a lesser extent due to the higher layer charge. Vermiculites are trioctahedral with the general formula: Mg (x-y)/2(Mg, Fe^{2+})$_{(3-y)}$(A1, Fe^{3+})$_y$ ($Si_{(4-x)}$ Al_x)$O_{10}(OH)_2 \cdot nH_2O$ (Reeves et al., 2006).

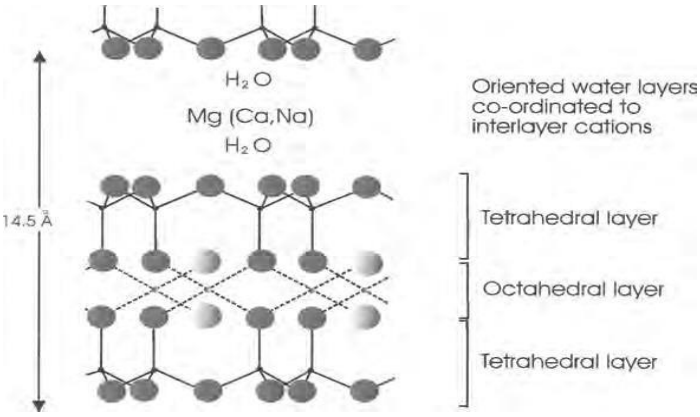

Figure 2.5: Crystal structure of vermiculite

2.2.1.2 Feldspar

Feldspars are the most abundant rock-forming minerals that makeup 60 % of the earth's crust. All the rock-forming feldspars are alumino-silicate minerals containing varying proportions of potassium and sodium or calcium. They are the most abundant minerals of igneous rock. The common feldspars are potash feldspar, namely orthoclase ($K_2O.Al_2O_3.6SiO_2$), meaning straight fracture. A variety of crossed, hatched, twinned orthoclase known as microcline ($K_2O.Al_2O_3.6SiO_2$), also known as "small incline," soda feldspar is called albite ($Na_2O.Al_2O_3.6SiO_2$). Lime feldspar is anorthite ($CaO.Al_2O_3.2SiO_2$) or plagioclase known as "oblique fracture" (Aliyu et al., 2016).

There are two sub-groups of feldspars, the alkali (or K-feldspar) and the plagioclase series. Isomorphism occurs between end-members (orthoclase, albite, and anorthite) of these series, indicated in the triangular phase diagram in Figure 2.6. The alkali feldspars show a continuous composition series between end members orthoclase ($KAlSi_3O_8$) and albite ($NaAlSi_3O_8$) for feldspars stable at high temperatures. However, the plagioclase series is continuous between end members albite ($NaAlSi_3O_8$) and anorthite ($CaAlSi_3O_8$) at all temperatures (Deer et al., 2001; Kyonka & Cook, 1954). A triangular phase diagram describing the compositions of the Feldspars is presented in figure 2.6 from (Deer et al., 2001).

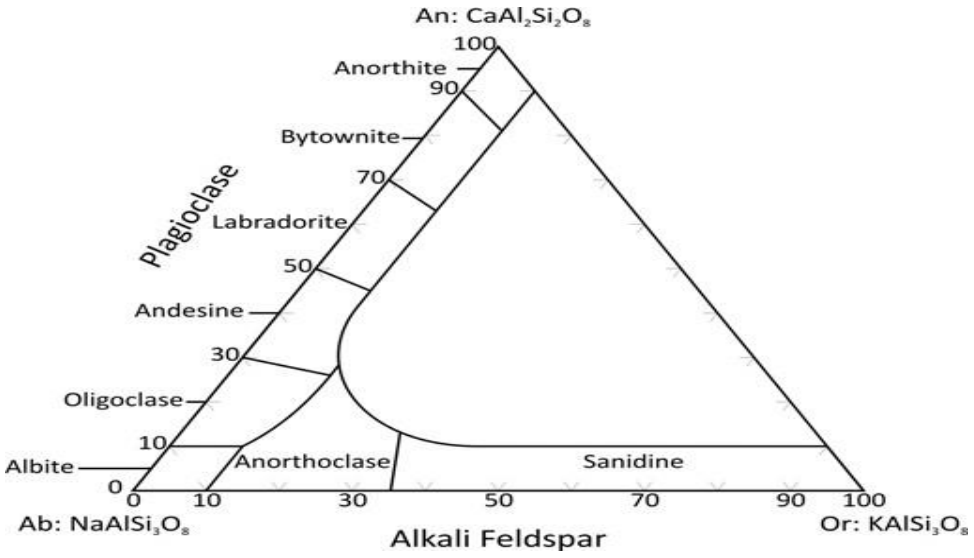

Figure 2.6: Triangular phase diagram describing the compositions of the Feldspars.

The amount of orthoclase and albite determines the quality of Feldspar in the Feldspar, the most commonly used fluxes in porcelain composition. Nowadays, mixed feldspars are considered suitable fluxing agents for porcelain manufacture. They develop a very dense glassy phase that embeds the new forming crystals and a part of the residual crystals present in the microstructure that enhances the densification process. Secondly, the mixed Feldspar minimizes the effect of changes in mineralogical mining (Mathur et al., 2015).

2.2.1.3 Quartz

Silicon dioxide is a complex material in many polymorphisms, where the most common stable conditions of silicon dioxide are quartz, cristobalite, and tridymite. The stable form is quartz at room temperature, between 870 and 1470 °C; the stable form is tridymite, while 1470 °C to the melting point 1713 °C, cristobalite is stable (Heaney & Veblen, 1991).

Silica is available naturally in various forms, as discussed above, and the most important is quartz. Quartz is the most common mineral found on the surface of the Earth. It is estimated that about 12% of the Earth's crust is made of quartz and is considered the most stable mineral under conditions at or near the surface. The primary source of quartz is sandstone. Quartz is composed of Silica tetrahedral grouped in such a way to form spirals with all the tetrahedral oxygen bonded to silicon (refer to Figure 2.7) from (Silberberg, 2013).

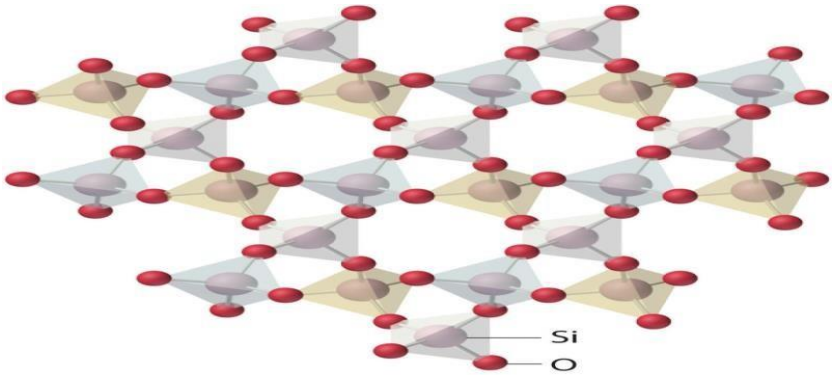

Figure 2.7 Crystal Structure of Quartz

Quartz exists in two forms, α, and β quartz. The α-quartz is stable up to 573 °C and β-quartz above this temperature. The α↔β inversion is reversible. The conversion from α-quartz to β-quartz is quick and accompanied by expansion and slight energy absorption (endothermic transformation). The inversion from β-quartz to α-quartz that occurs at 573 °C during the cooling stage is accompanied by shrinkage. Thus, the ceramic materials containing quartz should be processed carefully at this inversion temperature (Heaney & Veblen, 1991).

2.2.2 Important Properties of Raw Materials for Porcelain Insulator Production

2.2.2.1 Plasticity of Clay Minerals

Plasticity, in this case, and particularly in clay mineral systems, is defined as "the property of a material which allows it to be repeatedly deformed without rupture when acted upon by force sufficient to cause deformation and which allows it to retain its shape after the applied force has been removed" (Andrade et al., 2011). The plasticity of Clay depends on the clay-water system, a clay that shows maximum plasticity has optimum water content. A decrease in plasticity is observed at higher or lower water contents due to the rapid change in the system's extensibility (W. Lawrence, 2006). The high plasticity requires more force to deform it and deforms to a greater extent without cracking than low plasticity, which bends more easily and ruptures sooner (Andrade et al., 2011). As a rule, optimal plasticity can be considered as the minimum plasticity required for the moulding process to be performed satisfactorily, without any subsequent deformations or problems involving low mechanical strength in the green or dry pieces arising (W. Lawrence, 2006). In general, increasing plasticity in Clay is due to the presence of minerals in which the layers are weakly bound (minerals of montmorillonite), the reducing size of the particle, and the

presence of an organic substance (e.g., ball clay) (Andrade et al., 2011; Manfredini & Hanuskova, 2012).

Clay minerals with weak interlayer force and very fine particle size like montmorillonite, halloysite, and ball clays absorb a high amount of water in the interlayer and quickly swell and belong to the upper range plasticity. This kind of clay minerals nature possesses a potential hazard of cracking during fabrication (Akwilapo & Wiik, 2003). During the drying stage, it loses the water content present in the interlayer as it produces a high level of shrinkage. Additionally, such kinds of clay minerals can take a week to dry a green body. Still, kaolinite and illite minerals have intermolecular solid attraction forces between the layers. They exhibit moderate to low plasticity. They can dry quickly and result in slight shrinkage (Valásková, 2015); thus, kaolinite and illite favour porcelain ceramic fabrication.

2.2.2.3 Mullite in Pure Clay

Mullite is an aluminosilicate refractory material with various attractive properties, such as low thermal expansion, a high melting point, high thermal stability, low dielectric constant, high thermal shock resistance, and chemical stability. Due to these properties, the mullite phase is primarily targeted in the production of porcelain insulators. It is the only stable crystalline phase in Al_2O_3-SiO_2 systems with the chemical formula $3Al_2O_3 .2SiO_2$ (Hossain et al., 2018).

Early studies revealed the importance of the extent of mixing during the production of porcelain. Micro-regions of varying composition are present in the unfired ware, including pure clay agglomerates and feldspar-enriched regions. On heating, these regions react to form different types of mullite. Mullite crystals derived from the pure Clay (kaolin) agglomerate relicts are cuboidal and are referred to as primary mullite (2:1 type-mullite) since they form at the lowest temperature. Elongated needle-shaped mullite crystallizing from the feldspar-rich melt is termed secondary mullite (2:1 type-mullite) since it forms later in the firing process. The third form of mullite has been detected in porcelains containing alumina as filler termed tertiary mullite (Lee & Iqbal, 2001).

Generally, kaolinite and illite improve mullite formation (K. Dana & Das, 2003; Manfredini & Hanuskova, 2012). Because of the high level of alumina or low ratio of the level of SiO_2: Al_2O_3 whereas due to low alumina content in montmorillonite less favors the formation of mullite (Merga et al., 2019).

2.2.2.4 Quartz and Feldspar Particle Size

Feldspar and quartz are termed "non-plastics" because they possess no intrinsic plasticity by themselves. The function of non-plastic materials is twofold: (i) They are added to clays that are too plastic (having too significant a proportion of colloidal particles) to reduce plasticity and thus eliminate cracking, or distortion during drying and firing, and (ii) Non-plastic materials make it possible for the desired properties to be obtained at lower firing temperature (Mark & Onuoha, 2018).

A porcelain insulator can be improved by achieving the particle size of raw materials that must be controlled. The milling process is generally used to manage the raw materials particle size, which can improve the resulting properties of the green and sintered material. Smaller grain sizes for the quartz and Feldspar enhance the homogeneity of the vitreous phase and produce a more homogeneous structure for the sintered material (Andreev & Zakharov, 2009). But, when comparing the effect of Feldspar with quartz, the quartz particle size effects are relatively more pronounced than those of Feldspar because at the high sintering temperature, dissolution of a high amount of quartz results in an increase in a glassy phase and micro-cracks. It is also supposed that these micro-cracks occur during the β to α transformation of undissolved quartz grains, which is accompanied by relatively large volume shrinkage ($\Delta V/V=0.68\%$ for free quartz grains) at a temperature range of about 573°C. These conditions and relationships cause the micro-cracks around the grains (Boussouf et al., 2018). These cracks finally reduce the porcelain insulator's electrical and mechanical strength.

Generally, reducing the grain sizes of the quartz and Feldspar increases the amount of vitreous phase and increases the final shrinkage (reduces the porosity), and also reduce the expansion coefficient and smooths out the volume changes on the β to α quartz polymorphic transition (Andreev & Zakharov, 2009).

2.2.2.5 Raw Material Purity

Clay and Feldspar also contain small amounts of oxides, such as Na_2O, CaO, MgO, TiO_2, and Fe_2O_3, which may influence the body's crystallization behavior and verification temperature and glass viscosity (Iqbal & Lee, 2000). The impurities reduced the compactness of ceramic, and

overall porosity is as high as 15%, which causes a significant reduction in material strength and deterioration of its dielectric property (Gao et al., 2015; Kyasager & Prasanna, 2016).

A. Effect of Iron Compounds

For electrical insulation should have a high electrical resistivity that minimizes the energy conducted. In addition to electrical resistivity, the Porcelain insulator should exhibit the smallest possible dielectric constant (or relative permittivity) and loss tangent value. According to the study of (Piva et al., 2013), the presence of iron oxide in aluminous porcelains increased the dielectric constant. When hematite was present in amounts (1–3wt %), dielectric loss showed a minimum. Above 3wt% concentration of Fe_2O_3 increased the loss tangent, which rises with temperature and frequency. Loss tangent can be admitted to be invariant for lower Fe_2O_3 contents. The heating of the insulator due to dielectric loss caused by the presence of Fe_2O_3 may be a risk factor in the case of insulators used at high temperatures and low frequency. (Iqbal & Lee, 2000) also suggested that at elevated temperature, the decomposition of iron oxide occurred $3Fe_2O_3 \rightarrow 2Fe_3O_4 + {}^1/_2O_2$. The release of oxygen gases enclosed in the pore (called bloating) decreases bulk density (Akwilapo & Wiik, 2003). The Fe oxides are susceptible to oxidation-reduction reactions, which lead to color changes and glazing temperatures. Fe_3O_4 in combination with silica starts glass formation at temperatures of 1455°C. If it gets reduced to FeO, then glass formation can begin at a much lower temperature of 1180 °C. Fe_2O_3 and FeO are red and black, respectively, and confer these colors on clay products (W. G. Lawrence & West, 1982).

B. Effect of Calcium Compounds

The calcium compounds found in clays include calcite, aragonite, $CaCO_3$, and gypsum $CaSO_4.2H_2O$, which decompose on heating to form CaO, which acts as a flux. This then results in glass formation and lowers vitrification temperature. It increases the fired strength and reduces the absorption of the product. Cao combines with iron minerals and bleaches the red color to buff. If not fired to sufficiently high temperatures, CaO may remain as free lime, which reacts with water after firing to form $Ca(OH)_2$, which causes significant expansion and may develop sufficient pressure to disrupt the fired product (lime popping) (W. G. Lawrence & West, 1982). In addition to this, certain minerals like dolomite modify the reactivity of clay material and specifically lead to the formation of aluminosilicate of calcium, which inhabits mullite formation and enables

consolidation at low temperature with the appearance of the porous product (Manfredini & Hanuskova, 2012). So, there presence a negative effect on the final product.

2.2.2.6 Availability of the Raw Materials

The availability of raw material used to produce electrical porcelain insulators is the primary factor for the final production cost. For instance, in Nigeria, it has been estimated that more than 20% of the total outlay for a typical transmission and/or distribution system of electric energy is spent on insulation alone and prominent among them is porcelain. Nigeria imports almost a hundred percent of the total insulation it uses, of which porcelain occupies a central position, notably from the Asian countries (Ajakor & Ogwata, 2015). At the same time, according to (Merga A. 2018), the local manufacturer in Ethiopia to produce the electrical porcelain insulator applies foreign raw material (ball clay), which are imported finished product and indirectly on imported raw material for the domestic demand of overhead insulators. But it is evident that such a state of affairs adversely affects the country for exchange reserve and is inconsistent with the driving force for local substitution of imported goods (Ajakor & Ogwata, 2015) to save the foreign currency and finally to reduce production cost.

2.2.2.7 Chemical Composition of Feldspar

Feldspar is one of the essential materials that improve the properties of the mechanical porcelain product. The chemical and structural behaviour of feldspar material is the result of weathering stage of the original deposit. A feldspar composition that is found at an early stage of geological transformation consists of higher alkaline (K_2O +Na_2O) content which low level of Al_2O_3 due to its un-weather nature of the rock, but feldspar deposit found in a more advanced stage of geological condition transformed to kaolinite clay as a result of weathering, which contain a relatively low level of alkaline and consequently its fluxing behavior is reduced. However, a feldspar that can be applied for porcelain insulator fabrication must have alkaline oxide (K_2O +Na_2O) a minimum of 12 wt.% to obtain sufficient liquid or glassy phase required in the microstructure of porcelain body at economic firing temperature (Moyo & Park, 2014). On the other hand, its increase negatively affects the insulation and properties of porcelain affected by the concentration and quality of oxides (Na^+, K^+) for containing alkali metal ions because it is known that the dielectric constant of porcelain increases in the presence of K^+ and Na^+ cations and decreases when Ca^{2+}, Mg^{2+} replace them, and Ba^{2+}cations (Belhouchet et al., 2019).

2.2.3 Alternative Source of Porcelain Insulators Raw Material (Feldspar and quartz)

As discussed in section 2.2.1, Feldspar and quartz are generally the most useful in manufacturing porcelain insulator production. In other ways, the substitution of the natural Feldspar and quartz by another renewable material such as waste material has advantages both in quality and cost of the produced product.

In recent times, industrial activities generate vast amounts of solid wastes, which cause considerable environmental and economic problems. For this reason, industrial solid waste management ecologically and economically has become a matter of high global interest. Solid waste management strategies are currently focused mainly on reuse instead of elimination or storage of waste. Therefore, the ceramic industry, specifically the porcelain electrical insulator industry, is a well-established field for the reuse of solid wastes. This approach has environmental and economic advantages because the solid waste is incorporated into ceramic formulations in non-renewable natural raw materials (Schettino et al., 2016).

Silica/quartz is commonly used as the filler in porcelains because of its abundance and economy. However, silica or quartz is detrimental to porcelain insulator products because extensive cracking often results from the abrupt expansion changes accompanying phase transitions and the differences in expansion between the glass matrix and the quartz itself (Warshaw & Seider, 1967). Cracking occurs when β to α phase inversion of quartz occurs at 573°C during cooling. The inversion results in a decrease of quartz particle volume and may lead to cracks in the body (P. Olupot et al., 2014). For porcelain, the quest over the period has been to increase mechanical strength and reduce production costs. In most efforts to increase strength, emphasis has been placed on minimizing quartz in the porcelain formula. So far, there are reports of improvements in the mechanical properties by reducing/eliminating the use of quartz. Some of the reports on the replacement of quartz by waste materials are; rice husk ash, sillimanite sand, fly ash, silica fume, etc. (Jamo, 2015)

Feldspar is a commonly used fluxing mineral in standard porcelain bodies (Carty & Senapati, 2005). Due to the resources of high-grade feldspar minerals have recently begun to become depleted, and among the three raw material of porcelain insulator, Feldspar is the most expensive; thus, it is necessary to evolve an alternative source of fluxing materials for porcelain bodies, which

can serve to lower the temperature at which the viscous liquid form. On the other hand, its replacement would represent a significant reduction in final costs. Some of the studies on the substitution of Feldspar are; waste glass, blast furnace slag, sugarcane bagasse ash, etc. (Jamo, 2015)

2.2.4 SCBA as Fluxing Agent (Feldspar)

There have been remarkable increases in agricultural, industrial, and economic growths in the recent decades that have contributed to integrated improved quality and well-being for citizens. Hence, sugar factories are agro-industries that use sugarcane as the primary raw material and generate vast waste worldwide. Sugar cane is a commonly grown tropical and subtropical crop and is the main sugar crop worldwide. The global sugar crop average is approximately 31.3 million hectares, among which sugar cane accounts for about 70% (Xu et al., 2018). Brazil is the world's largest producer of sugarcane, followed by India, China, and Thailand. Likewise, Ethiopia is on the way to have about 15 sugar factories within a few years in which all generate massive amounts of sugarcane bagasse, as shown in the table. However, this increasing number of sugar industries gave rise to new problems related to dumping vast quantities of solid waste byproducts such as Sugar Cane Bagasse Ash into the environment. The Brazilian sugarcane industry alone generates around 4 million tons per year of SCBA. The estimated quantity of bagasse ash produced from Ethiopia's sugar industries may reach up to two million tons per annum (Mosisa et al., 2019).

The SCBA waste has negligible costs and is easily overlooked in landfills, which can significantly cause severe environmental and human health concerns unless it is appropriately managed. For instance, inhalation of dust from the disposing of Bagasse ash can cause chronic respiratory disease. Moreover, improper land disposal of Bagasse ash in a dry season is vulnerable to wind and increases the quantity of dust in the ambient air (Frias et al., 2011). So far, the final solution for this solid waste can be mainly used in the ceramic industry to fully or partially replace the natural raw material (Mosisa et al., 2019).

SCBA is termed an aluminosilicate because of silica (SiO_2) and alumina (Al_2O_3). Thus, SCBA waste is similar in chemical composition to common natural aluminosilicate porcelain raw material (Feldspar for this study) used to produce porcelain insulators. This means that the reuse of SCBA waste as a possible raw material for porcelain insulators is an essential technological solution. This

approach has environmental and economic advantages because the solid waste is incorporated into ceramic formulations in non-renewable natural raw materials (Schettino et al., 2016).

Some works on the incorporation of SCBA acts as a fluxing agent in ceramic bodies ((Teixeira et al., 2014); (Tonnayopas, 2013); (Souza et al., 2011); (Hariharan et al., 2018)). From those studies, Hariharan et al. investigated the preparation and characterization of ceramic products with sugarcane bagasse ash waste. The final result of this study shows that the partial substitution of SCBA on the porcelain insulator composition results in a reduction in water absorption and porosity and an increase in its bulk density and dielectric strength. The microstructure revealed a reduction in pores and revealed a denser matrix with the advent of vitrification.

2.3 Industrial Manufacturing Process of Porcelain Electrical Insulator

The manufacturing process of porcelain insulators has many steps (Refer to Figure 3) (Ash & Chandrasekhar, 2017). It has a reasonably long process cycle ranging from 15 days to 21 days. Adding to this long process cycle, porcelain insulators have to pass through almost 35 process steps. Each process steps have its importance and contribute to the quality and performance of the insulators. It transforms raw, earthy materials like Clay, quartz, and Feldspar into electrical equipment used in the electrical power system. It is then becoming the backbone of electrical power transmission and distribution systems as insulators. The manufacturing process of porcelain insulator is presented in figure 2.8 from (Ash & Chandrasekhar, 2017)

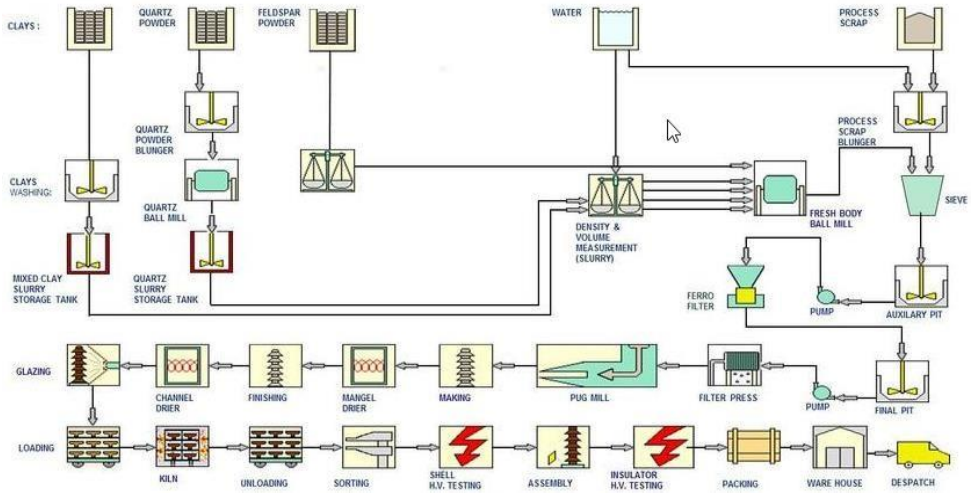

Figure 2.8: Manufacturing process of porcelain insulators

2.3.1 Obtaining and Preparing the Material

The first step in the manufacturing process of porcelain electrical insulator is mining, which is the process of obtaining the raw clays from surface pits or underground mines, natural minerals such as Feldspar and quartz that are used to lower the sintering temperature and maintain the dimensional stability and chemical additives needed for the shaping process. After the raw materials have been extracted, hard raw materials, such as feldspars and quartz, are reduced to the desired size by successively grinding through one or more jaw crushers and then to a ring mill for final sizing. Oversize particles are screened after ring milling and returned through the process in a closed-loop system. Most clay materials are not beneficiated at the plant site before blending or milling. Still, in some cases, especially where continuous ball milling is subsequently used, the clay portion of the body may be pre-blended in high-speed blungers to ensure dispersion or "slaking" of the clay particles before final blending or milling.

2.3.2 Milling

Weighed materials are fed to a collector belt which transfers the composite to a large ball mill. Water is automatically provided to the mill through a metering system also controlled by the computer. This portion of the process is by far the most crucial since the old saying of "garbage in, garbage out" is never truer than in the correct weighing and/or proportioning of raw materials in the first step of a ceramic process. The control of all raw materials is crucial for the continuous, smooth running of a plant.

Once the raw materials are prepared in the correct proportion, it is charged into a ball where crushing by the centrifugal action of the rotating mill and the balls take place. The mill is cylindrical and is made of stainless steel. Both the internal lining and the balls are made of ceramic-making materials to avoid product contamination. The particle size is the controlling parameter for proper milling. Sample from the mill is taken, and particle size is measured using a hydrometer method based on the principle that coarse particles settle faster under gravity.

2.3.3 Blunging

If the milling is acceptable, the mixture from the mill is emptied by the pipeline into the first blunger. The blunger is a large circular tank containing the exact amount of water required by the batch and is equipped with power-driven paddles to agitate the various ingredients of the batch.

Agitation is continued until the specific gravity of the slip has reached a required point indicating complete suspension of all the dry ingredients in the water, in other words, until the raw materials are disintegrated and suspended in the water. Although quite commonly used, this preparation method is inferior in many respects to grinding or even mixing in pebble mills. The function of the blungers is simply mixing and uniforming the body composition.

2.3.4 Sieving and Magnetic Separation

The slip from the blunger is directly transported to the vibrating sieves using compressed diaphragm pumps. The sieves are two in number, and they work in turn; while one is working, the other is cleaned. The sieves separate coarse particles from the slip, which is then dried and re-milled later. On the bottom of the vibrating sieves lie permanent magnets that separate iron and other magnetic materials that will otherwise produce spots and coloring problems upon firing. The fired slip is collected and stirred in two blungers D-1 and D-2 until transported to the casting room slip storage tanks H-1 and H-2. The slip is left to age before casting for about 24 hours.

2.3.5 Filter Pressing

The slip or raw porcelain is drained from the blunger by gravity over a jig table through 140-mesh screens, then flows over a magnetic separator to a pump that transports the slip to a storage cistern. Slip is pumped from the storage cisterns, as it is required, to these filter presses. Here the excess water is removed, leaving the Clay in round cakes containing approximately 25 percent water, thoroughly plastic, and ready for processing.

2.3.6 Pugging

Whether taken directly from the press or aged, Filter press cakes require a thorough mixing to produce better homogeneity. This is done in a pug mill, which thoroughly mixes the mass, develops plasticity, and eliminates any enclosed air. Proper pugging necessitates careful study as each body works differently and requires special attention.

2.3.7 Shaping-forming

Forming the plastic clay body into the finished insulator shape before the firing to vitrification is of great importance. The shaping method used depends on the type of raw material and, mainly,

upon water content and type of insulator required. Among the methods used to accomplish this are dust or Semi-dry Pressing, Plastic Forming, and Casting.

Dust pressed insulators are used chiefly in low-tension work. The prepared plastic body is dried out, dampened with a definite amount of water, pulverized, and pressed in steel moulds. The density of this product is not as great as that made in other ways but accurately sized; complex shapes can be made. Turning from pugged blanks, throwing and jiggering are processes in which the body is roughly shaped while in the plastic condition and might be termed "plastic forming." Pieces formed this way are trued up or fettled while still damp but stiff enough to hold their shape.

The most common method of shaping thin-walled insulators is with a hot press die. Here, the plaster of Paris mould, having the shape of the outside or top of the insulator, is placed on a horizontally revolving wheel. The plastic clay body is placed in the mould and carefully pressed down to conform with the mould. A heated metal part is forced down onto the Clay in the revolving mould and shapes the spinning Clay into proper form for the bottom of the insulator. The hot metal causes steam to be formed from the water in the plastic clay body, and this acts as a lubricant, preventing the Clay from tearing and making it possible to form extremely thin petticoats or walls.

Casting is done by preparing the clay body with sufficient water and electrolytes to form a liquid (slip). This is poured into dry plaster of Paris moulds of proper shape. The plaster absorbs water from the Clay and allows it to stiffen and become firm enough to be handled when the mould is removed after an appropriate time. An adequately prepared slip has no more water (hence no more shrinkage) than a plastic body. Pouring in the liquid condition makes it possible to form heavy pieces comparatively free from strains.

2.3.8 Drying Green Porcelain

Wet porcelain from moulding or cutting machines contains 7 to 30 percent moisture, depending upon the forming method. Before the firing process begins, most of this water is evaporated in dryer chambers at temperatures ranging from about 38 ºC to 204 ºC. The extent of drying time, which varies with different clays, usually is between 24 to 48 hours. Although heat may be generated specifically for dryer chambers, it is generally supplied from kilns' exhaust heat to maximize thermal efficiency. In all cases, heat and humidity must be carefully regulated to avoid cracking in the brick.

2.3.9 Drying

The wet porcelain coming from the shape-forming operation typically has moisture contents ranging from 5 to 20 wt%. This water is removed in dryers at temperatures ranging from 40 to 150°C over one to two days. The drying process is carried out in a series of chambers (intermittent dryers) or tunnels (continues dryers). The temperature and humidity of the air are regulated to control the shrinkage during drying. Most dryers recycle the hot air from the cooling zones of the sintering kilns.

2.3.10 Glazing

Glaze act as smooth, relatively thin glassy coating of ceramic body which is effectively bonded to its substrate. The main reason for the use of glazes as surface coatings of ceramic materials is their relatively high chemical resistance and aesthetic aspects. A glaze is usually formulated by mixing together the appropriate amount of finely-ground potter's (SiO_2), boric acid, feldspar (a source of K_2O, Na_2O, CaO and Al_2O_3) and whiting ($CaCO_3$) if required, a coloring agent. An appropriate mixture of these components, when made into slurry with water, can be painted onto the clay body and fired. The component will react together to form viscous liquid which becomes a colored glass.

2.3.11 Firing dried porcelains Insulator in a kiln

Firing is a crucial process in the manufacture of ceramic products, as it controls many essential properties of the finished ware. These include mechanical strength, abrasion resistance, dimensional stability, resistance to water and chemicals, and fire resistance.

The burning of the porcelains is a critical stage in the production process. Firing temperature and atmosphere will determine the ceramic properties, such as strength, porosity, size, and final product colour. Different types of kilns are used for firing porcelain insulators. Tunnel and continuous kilns are more recent innovations, and their use is increasing in porcelain insulator manufacturing. The cooling of the porcelain insulators normally requires 2 to 3 days in a continuous kiln and no more than two days in a tunnel kiln (Rahaman, 2017). However, the rate of cooling will affect the colour and strength of the ceramic. The changes in the structure of triaxial bodies during firing are not completely understood due to their complexity. Table 2.5 is an approximate summary of what probably occurs during the firing of a whiteware body (Norton, 1974).

Table 2.2: The life history of triaxial body

Temperature (°C)	**Reactions**
Up to 100	Loss of moisture
100-200	Removal of absorbed water
450	Dehydroxylation
500	Oxidation of organic matter
573	Quartz inversion to high form. Little overall volume damage
980	Spinel forms from Clay. Start of shrinkage
1000	Primary mullite forms
1050-1100	Glass forms from Feldspar, mullite grows, shrinkage continues
1200	More glass, mullite grows, pores closing, some quartz solution
1250	Glass 60%, mullite 19%, quartz19%, pores at minimum

2.4 Chemistry of Microstructure of Porcelain insulators

Porcelain microstructures are grain and bond types with a large grain or filler (usually quartz) held together by a finer bond or matrix. The gross microstructure of fired triaxial porcelain consists of quartz, Feldspar, and clay relicts in a glassy matrix. Mullite crystals coming from the clay relicts have a scaly appearance and are referred to as primary mullite. In contrast, the long needle-shaped mullite crystals crystallizing from the feldspar melt are termed secondary mullite (Iqbal & Lee, 2000). The basic reaction steps ignoring the removal of nonchemically bound species, such as water and organics, can be outlined as follows:

i. The crystal structure of kaolinite contains hydroxyl groups, and the dihydroxylation of these groups to form metakaolin ($Al_2O_3.2SiO_2$) occurs at around 550°C. The chemical equation representing this process is (Kausik Dana & Das, 2004a).

$$Al_2O_3 .2SiO_2 .2H_2O \text{ (kaolinite)} \rightarrow Al_2O_3 .2SiO_2 \text{ (metakaolinite)} + 2H_2O\uparrow$$

ii. Metakaolin transforms into a non-equilibrium spinel-type structure and amorphous free silica at approximately 950-1000°C. The amorphous silica liberated during the metakaolin decomposition is highly reactive, possibly assisting eutectic melt formation at around 990~ (Ajakor & Ogwata, 2015; Carty & Senapati, 2005).

$$2SiO_2\,Al_2O_3\,(\text{metakaolinite}) \rightarrow SiAl_2O_4\,(\text{spinel}) + SiO_2\,(\text{amorphous})$$

iii. The spinel transforms to primary mullite and silica at temperatures above 1100 ^{0}C. Due to this reaction series, primary mullite is commonly observed in porcelain microstructure as an aggregate of tiny crystals (<0.5µm) in the clay relicts. Secondary mullite forms by the reaction of clay relicts with feldspar relicts at around 1200 ^{0}C and it appears as a long needle (>1µm) shaped crystals (Iqbal & Lee, 2000).

$$SiAl_2O_4(\text{spinel}) + SiO_2\,(\text{amorphous}) \rightarrow \tfrac{1}{3}\,3Al_2O.2SiO_2\,(\text{mullite}) + \tfrac{4}{3}SiO_2\,(\text{amorphous})$$

iv. Above 1200^{0}C, the mullite and amorphous silica producing mullite and free silica in the form of cristobalite (Ajakor & Ogwata, 2015).

$$3Al_2O.2SiO_2\,(\text{mullite}) + 6SiO_2\,(\text{silica}) \rightarrow 3Al_2O_3.\,H_2O\,(\text{mullite}) + 4SiO_2\,(\text{cristobalite})$$

v. Between 1250 – 1300 ^{0}C, feldspar dissolves the silica present in kaolin and that present in the mixture to form feldspar glass.

$$\text{Feldspar glass} + \text{mullite} + \text{cristobalite} \rightarrow \text{porcelain}$$

vi. On cooling, quartz inversion occurs at a temperature of 573 0C; this results in a decrease in the volume of the body by about 2%. Finally, the alpha to beta cristobalite inversion at 225-250 °C is similar to the quartz inversion, but it produces a larger volumetric change (5%); with a higher activation energy barrier, the transformation is less severe than that of quartz. (Carty & Senapati, 2005).

According to (Iqbal & Lee, 2000), the typical final microstructures of fired porcelain bodies consist of 10%-25% mullite, with composition ranging from $2Al_2O_3.SiO_2$ to $3Al_2O_3.2SiO_2$, 5-25% α-quartz (SiO_2), and 0-8% pores dispersed in 65-80% potassium aluminosilicate glass. Bodies with a high percentage of quartz also may contain cristobalite.

2.5 Effect of Microstructure on the Technological Properties of Porcelain Insulator

The development of porcelain's physicomechanical and dielectric properties is contributed by each phase developed during firing, which depends on the concentration and microstructural attributes influenced by temperature and the chemical composition of the raw materials (Ngayakamo & Park, 2018). Major determinant phases produced during porcelain production are mullite ($Al_6Si_2O_3$) and unresolved quartz (SiO2) crystal embedded in a continuous glassy phase originated from feldspar and other low melting impurities in the raw materials (Kitouni, 2014).

2.5.1 Physical Properties

The physical properties (bulk density, apparent porosity, and water absorbance) of porcelain electrical insulators depend on the microstructure and the phase distribution developed during the firing process. These two properties rely on the chemical composition of the raw materials, the preparation method, and the time and temperature of firing (Akwilapo & Wiik, 2003). The glassy phase derived from feldspar and quartz component in the porcelain composition has a dominant influence on the physical properties of fired ceramics. The glassy phase or liquid derived fills the gaps and void in the microstructure, which leads to densification of the body; thus, the ceramic body becomes denser, and its water absorbance and apparent porosity will decrease (Iqbal, 2008). However, an excess quantity of glassy phase leads to blotting phenomena at high firing temperatures that form small pore or void space, leading to increasing porosity and lower final product quality (P. Olupot, 2006).

2.5.2 Electrical Properties

The dielectric of porcelain electrical insulator is affected by the phases which are developed on sintering. Phases which are important for proper electrical insulation are mullite and glassy phase. Mullite phases, particularly the needle-like shape, proved to perform well in electrical insulation property. On the other hand, excessive glassy phase existence promotes free movement of ions hence poor electrical insulation properties (Islam et al., 2004; Moyo & Park, 2014).

2.5.3 Mechanical Properties

The mechanical properties of porcelains are largely dependent on their microstructure. The microstructure is developed during ceramic processing. The main factors that can affect the

mechanical strength of porcelain are coefficient of thermal expansion, mechanical properties of the present phases, homogeneous distribution of particles in the glassy phase, the particle size of the crystalline phases, the volume fraction of the present phases, and the phase transformations (Manfredini & Hanuskova, 2012). The effects of the individual phases on the mechanical properties have been elucidated under the mullite hypothesis, the matrix reinforcement, and the dispersion strengthening hypotheses detail explained by (Carty & Senapati, 2005).

Mullite's hypothesis suggested the strength of the porcelain material was solely dependent on the interlocking fine mullite needles. Growth of the strength was later attributed to an increase in mullite content. The mullite ($3Al_2O_3 \cdot 2SiO_2$) is characterized by good mechanical, electrical, and chemical properties. It is resistant to thermal shocks as well. Hence, it has been argued that the strength grows with the increase of this phase content. The smaller needles can interlock more efficiently than the larger ones. As a result, the temperature of firing and generating the suitable amount of correctly sized needle-shaped crystals of mullite is crucial to achieving higher strength. Small needle crystals of secondary mullite can increase strength more effectively than scaly crystals of primary mullite.

The matrix reinforcement hypothesis states that the difference in thermal expansion coefficients between the matrix (glassy phase) and dispersed particles (such as quartz) or crystalline phases formed during firing (such as mullite and cristobalite) produces solid compressive stresses on the glassy phase. The larger these stresses are, the higher is the strength of the porcelain body. The phenomenon is known as the pre-stressing effect. This theory is related to the function of the quartz phase in the porcelain body. Moreover, the nature of cracks in porcelain bodies is dependent on the expansion coefficients of the matrix and the particle. If the particles contract more than the matrix, resulting in circumferential cracking around the particles. This is true for quartz particles in the feldspathic glass matrix of the porcelain body. The stress generation and associated cracking due to the presence of quartz particles tend to be severe because of the rapid displacive phase transformation of quartz during cooling

The dispersion-strengthening hypothesis states that dispersed particles in the vitreous phase of a porcelain body, such as quartz and mullite crystals in the glassy phase, limit the size of Griffith flaws resulting in increased strength. This hypothesis deals with the homogeneity of phases throughout the body achieved by sufficient mixing in the production process.

Some of the evidence supporting the above three hypotheses (Islam et al., 2004) concludes that the best mechanical and dielectric properties can be achieved by high mullite and quartz content with the low amount of the glassy phase in the absence of microcracks. A high amount of SiO_2 leads to a high amount of the glassy phase, which is detrimental to the development of high dielectric strength. An increase of the glassy phase gives an increased length of the free path of mobile ions like Na^+, $k^{+,}$ and $A1^{3+}$, increasing the conductivity. Another evidence shows that under optimized conditions of firing and for particle size of 10-30µm, quartz has a beneficial effect on the strength of porcelain, in conformity with the matrix reinforcement and dispersion strengthen hypothesis (P. Olupot et al., 2014).

2.6 Theory of Techniques Used in this Thesis

2.6.1 Atomic Absorption Spectrometry (AAS)

The atomic absorption spectroscopy (AAS) analysis of the primary raw material (kaolin, feldspar, and quartz) and waste material (SCBA) samples are intended to find out the concentration of the major and minor oxides in the deposit. This helps identify significant impurities, estimate the combination of phases resulting at high temperatures, and determine their ceramic potential for porcelain insulator production. In atomic absorption spectroscopy, emission, absorption, and fluorescence energy are put into the atom population by thermal, electromagnetic, chemical, and electrical forms of energy. It is converted to light energy by various atomic and electronic processes before measurement. It is beneficial not only for the identification but also for the quantitative determination of many elements present in samples (Bader, 2011). Baker and Suhr give the principle of involvement. When an atom is excited by thermal energy or other energy sources, they emit radiation by dropping down to less energetic states or the ground states as atoms always try to be an in-ground state at all times. This can be given by the following equation 2.1 (Baker & Suhr, 2015):

$M + hv \rightarrow M^*$

Absorption

Where M is the neutral atom, M* is the excited atom, h is Planck's constant, and v is the frequency.

2.6.2 X-Ray Diffraction (XRD)

XRD is most widely used to identify unknown crystalline materials (e.g., minerals, inorganic compounds). XRD measures the intensities of a reflected area from a small space, and from the results obtained, the atomic-level spacing of the crystal can be calculated. This helps in understanding the crystal structure of the substance. Determination of the degree of crystallization can also be calculated with the help of XRD. Furthermore, XRD also helps identify different phases with identical compositions, such as the state of atomic order. Due to this versatility, XRD is one of the most commonly used devices in the industrial world and research because of its simplicity and ease of use.

The X-ray diffraction technique is based on the following principle. When an X-ray beam falls on equally spaced atoms of a crystalline mineral, they are transmitted, absorbed, or scattered. When scattering, they can be scattered coherently (without energy loss) or incoherently (with energy loss). The coherently scattered light will form an interference pattern when the scattering centers are arranged regularly. The distance between scattering centers is comparable to the wavelength of the light. This phenomenon is called diffraction (Amonette, 2002).

X-rays behave as waves that interfere with each other, i.e., waves in phase reinforce each other while waves out-of-phase weaken each other. A reflection is formed only when the reflected X-rays are in phase with each other. In other words, Bragg's law (given below) must be satisfied (Atkins, 1996).

$$n\lambda = 2d \sin(\theta) \quad \text{.....(2.1)}$$

where n is an integer, λ is the wavelength of the X-rays, d is the distance between the Miller layers in the structure, and θ is the angle of the incident X-rays. The reflected beams are in phase if the extra length (BC + CD) traveled by the lower wave is an integer multiplied by the wavelength of the X-ray, see Figure. 1.9 from (Chang, 2005).

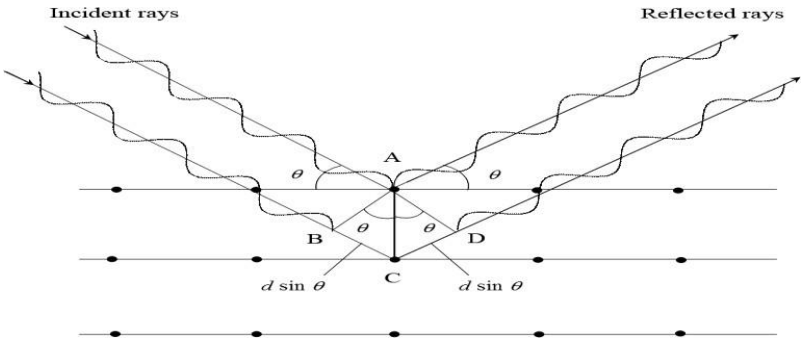

Figure 2.9. Reflections of X-rays from two layers of atoms.

2.6.3 Thermal Analysis (TA)

Thermal analysis is the general name for several methods, which are used for the investigation of the thermal properties of a material. In this technique, mineral identification is achieved by evaluating the weight loss and enthalpy changes in the soil sample with temperature. The most common methods used in TA are thermal gravimetric analysis (TGA), differential thermal analysis (DTA) and differential scanning calorimetry (DSC) (Amonette et al., 1994). Principles, setup, and output for common thermal analysis are presented figure 2.10 from (Amonette, 2002).

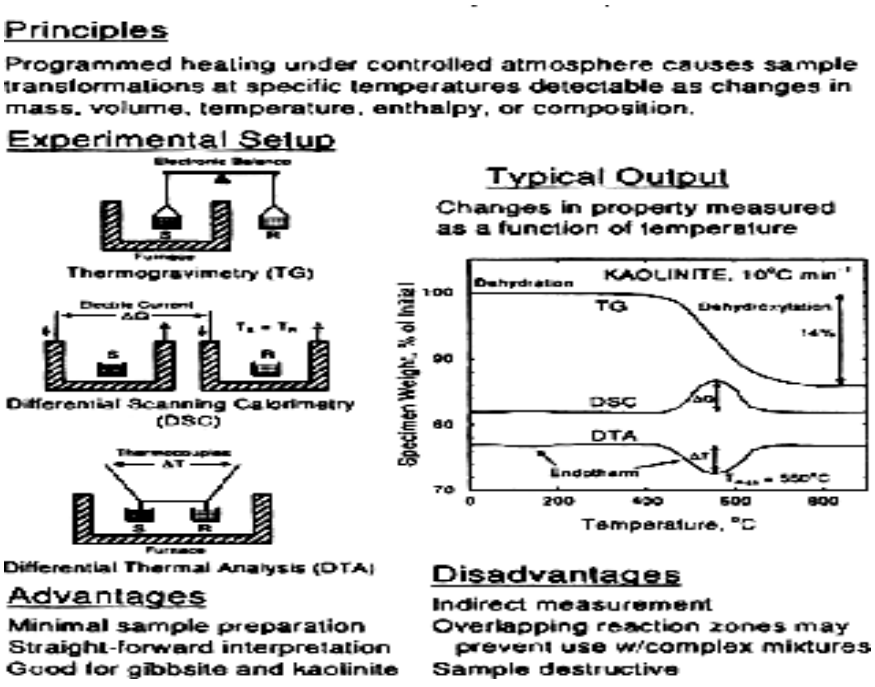

Figure 2.10: Principles, setup, and output for typical thermal analysis

Thermogravimetric analysis or thermal gravimetric analysis (TGA) is a type of testing performed on samples that determines weight changes to change in temperature. This can be used to determine how much of a substance was lost at a particular temperature or over a temperature range where a reaction takes place, such as dehydroxylation (Xi et al., 2005). The measurement is usually carried out in air or an inert atmosphere, such as helium or argon, and the weight is recorded as a function of increasing temperature. This method is used primarily to determine the chemical composition of the material because different reactions (such as oxidation or dehydration) during the heating process up to a temperature of 1000°C can occur. The material's thermal stability, the chemical composition of clay, oxidative stability, and kinetics of the decomposition of clay can be obtained from that method. In addition, the nature of evolving gases can be investigated. TGA is a qualitative and a quantitative method (Bish & Duffy, 1990).

The differential thermal analysis compares the temperature difference between the sample and thermally inert reference material when subjected to the same atmospheric conditions and heating rate. The changes in the weight of the samples during the heating process are related to the emission or absorption of energy. They are visualized by endothermic or exothermic peaks of the DTA (differential thermal analysis) graph. For clays, endothermic reactions involve desorption of surface H_2O (e.g., H_2O on exterior surfaces) and dehydration (e.g., interlayer H_2O) at low temperatures (100°C), dehydration, and dehydroxylation at more elevated temperatures, and, eventually, melting. Exothermic reactions are related to recrystallization at high temperatures that may be nearly concurrent with or after dehydroxylation and melting. Therefore, a typical DTA plot consists of a horizontal line (corresponding to a temperature difference of nil) with peaks or dips at specific temperatures where exothermic or endothermic reactions occur.

The third method is Differential Scanning Calorimetry (DSC), used to determine organic compounds in the sample. This technique monitors the thermal flux variation of material compared to the inert reference (conditions for sample and reference). It is a qualitative and quantitative method.

2.6.4 Plasticity Analysis

2.6.4.1 Atterberg Limit

The consistency of fine-grained soil is influenced mainly by the water content of the soil. A gradual decrease in water content of a fine-grained soil slurry causes the soil to pass from the liquid state to a plastic state, from the plastic state to a semi-solid state, and finally to the solid state, as shown in Figure 2.11. The water contents at these changes of state are different for different soils. When adding water to soil changes its consistency from hard and rigid to soft and pliable; the soil is said to exhibit plasticity. The water contents that correspond to these changes of state are called the Atterberg limits. The water contents corresponding to a transition from one state to the next are known as the liquid limit, the plastic limit and the shrinkage limit (Roy & Kumar Bhalla, 2017). Consistency of cohesive soils from is presented in figure 2.11 from (Das, 2008)

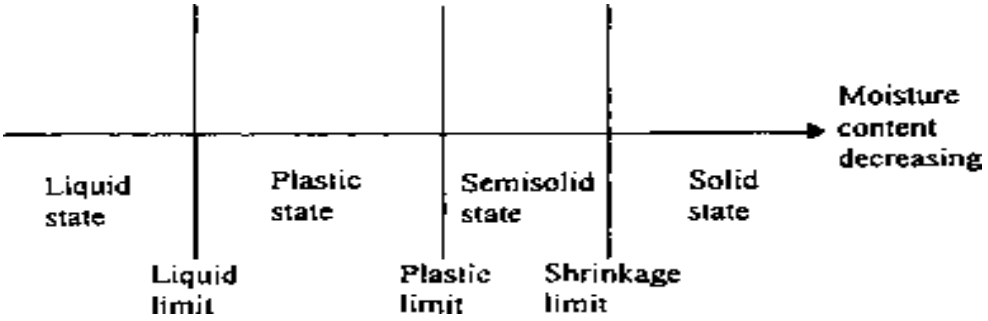

Figure 2.11 Consistency of cohesive soils

The liquid limit of soil is the water content, expressed as a percentage of the weight of the oven-dried soil, at the boundary between the liquid and plastic states of consistency of the soil. In contrast, the plastic limit (PL) is the water content, expressed in percentage, below which the soil stops behaving like a plastic material. It begins to crumble when rolled into a thread of soil of 3.0mm diameter. The soil in the plastic state can be remoulded into different shapes. When the water content has reduced, the plasticity of the soil decreases, changing into a semisolid state, and it cracks when remoulded. The difference between the Liquid Limit and the Plastic Limit of a soil is termed plastic index (PI). The Plasticity Index is an important parameter in classifying fine-grained soils. It is the basis of the Casagrande plasticity chart and, ultimately, the Unified Soil Classification System (Das, 2008). The more plastic or (higher plastic index value) a soil means

the more comprisable, higher shrinkage – swell potential, and the lower is its permeability (Abramson et al., 1995).

Atterberg classifies the soils according to their plasticity indices (PI), for non-plastic soils PI=0, for low plastic soils PI<7, for medium plastic soils PI between 7 and 17, and highly plastic soils PI>17 (Celik, 2010).

Table 2.3. Types of soils based on plasticity index

Plastic index	Degree of plasticity
0	Non-plastic
<7	Low-plastic
7-17	Medium-plastic
>17	High-plastic

2.6.5 Grain Size Distribution Analysis

The particle size distribution is used to distinguish the particle size and the major portion of the particle size and characterize the soil. Grain size analysis helps describe a wide variety of physical properties and affect porosity and permeability, and they are also related to the geotechnical properties of sediment (Boggs, 1995). This test is performed in two stages: sieve analysis for coarse-grained soils (Sands, gravels) and hydrometer analysis for fine-grained soils (clays, silts). Soils containing both types are tested in sequence, with the material passing the No.200 sieve (0.075 mm or smaller) analyzed by hydrometer.

Most granular soils and fine aggregates are mixtures of desirable coarse particles, sand, and undesirable clay or plastic fines. The sieve analysis test, which can also be referred to as grain size test or sand equivalent test which is intended as a rapid field correlation test to indicate the relative proportions of clay-like or plastic fines and dust in granular soils and fine aggregates that pass the No. 4 (4.75 mm) sieve size. This test provides a direct measurement of soil particle size distribution by causing the sample to pass through a series of wire screens with progressively smaller openings of known size. The amount of material retained on each sieve is weighed.

The hydrometer analysis, also called the sedimentation method, is based on soil sedimentation. It is used to determine the grain size distribution for a fraction of the soil that is smaller than the No. 10 sieves. Fine soil particles are dispersed by soaking the soil sample in a dispersing agent and by rapid stirring to neutralize the charges between the soil particles. A hydrometer test is used to determine what type of clay is predominant in a given soil sample (e.g., kaolinite, illite, montmorillonite, etc.). According to ASTM standard, soil can be classified as gravel, sand, silt, and clay based on the grain size as indicated in the table

Table 2.4: Soil classification system based on ASTM standard

Grain size (mm)			
Gravel	Sand	Slit	clay
2.00 – 100	0.075 – 2.00	0.005 – 0.075	< 0.005

3. METHODS AND MATERIAL

3.1 Materials and Equipment used for the experimental work

The following table shows the raw materials and equipment used during the experimental works.

Table 3.1: The raw materials and equipment used during the laboratory works

Materials	Uses
Raw materials	
Clay	To form plastic property during molding
Feldspar	To form the liquid phase and to reduce firing temperature
Sand/quartz	To maintain shape stability of the material
SCBA	To reduce the firing temperature and improves the porcelain insulator quality
A small amount of water (7%)	For dry milling and facilitate clay plasticity during shaping
Equipment	
A different size sieves	For particle size distribution analysis.
0.01g sensitivity electronic balance	For weighing samples.
Ball mill	To homogenize mixing the raw and waste material mixture (batches).
Jaw crusher	To reduce the raw and waste material to desired sieve size.
Hydraulic press	To shape the milled powder to the desired dimension.
Furnace	To fire the shaped porcelain body
Micro-meter	To measure the dimension of the produced insulator test body.
Oven	For drying samples
Water bath with heater	For water absorption, bulk density, and apparent porosity tests.

Casagrande cup	For liquid limit test
Glass plate	For plastic limit test

3.2 Sample Collection and Preparation

The representative raw material (clays, feldspar, and quartz) in the present study was taken from the De-yuan ceramic factory found in the Dukem industrial park, Ethiopia. The selected raw materials were termed as simply as BC (clay from Bombawuha), DC (clay from Denkaka), AF (feldspar from Arerti), WF (feldspar from Wolkite), and CS (sand from Chancho). The original deposits are indicated on the map shown in Figure 3.1.

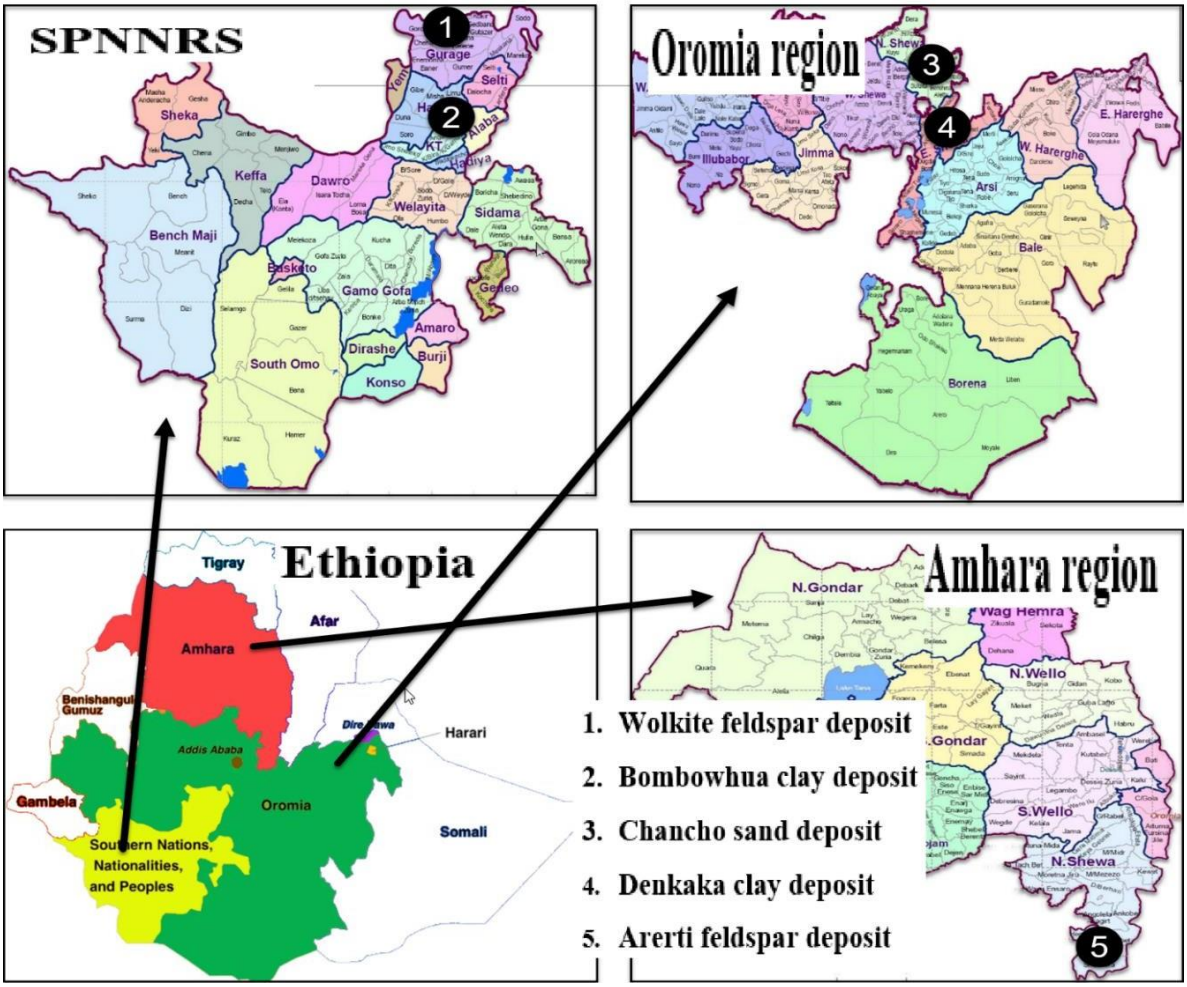

Where SPNNRS represents the south nation and nationalities regional state

Figure 3.1: Geographical location of the minerals studied

The collected and representative samples from each location and the waste material termed SCBA (sugarcane bagasse ash collected from wonji Shewa sugar factory) were crushed. They were ground separately, then clays, sugarcane bagasse ash (SCBA), and feldspar passed through 63μm opening Sieve, while quartz through 45μm. These samples were then used for all experiments.

3.3 Characterization of Raw Material Samples

The raw and waste materials were characterized with respect to their chemical compositions and mineralogy for both the waste material and raw material. Thermal property, particle size distribution, and plasticity were characterized for the two clays (BC and DC).

3.3.1 Chemical Composition Analysis

In this study, the chemical composition analysis of raw material (clay, feldspar, and quartz) and waste material (SCBA) was done by atomic absorption spectrometer (AAS) (spectry AA-20 plus) model at the Geological Survey of Ethiopia. Apart from the AAS, the $LiBO_2$ Fusion, HF attack, Gravimetric, Colorimetric were carried out for all samples to perform the complete silica analysis at the Geological Survey of Ethiopia.

3.3.2 Thermal Analysis

The changes in physical properties and/or reaction products when the raw materials are heated under controlled conditions were conducted using differential thermogravimetric analysis (TGA) following the procedure reported by (Mahmoudi et al., 2017). An oven-dried normal clay sample was used and analyzed using differential thermogravimetry (TGA) (Shimadzu DTG-60H, Japan) operating under inert atmosphere conditions. The samples were heated from room temperature to 1200°C in a Platinum/alumina cup with a heating rate of 10 °C/min, and an empty Platinum/alumina cup was used as control.

3.3.3 Mineralogy Analysis

The mineralogical analysis of all samples and phase analysis of the fried product was carried out using the XRD machine model of Shimadzu XRD-7000 X-ray diffractometer using Cu-Kα radiation (λ= 1.5418Å) using the operating voltage of 40 kV, a current of 30 mA, over the diffraction angle (2θ) range between 10° and 80°. The mineralogy of feldspar, quartz, and sugarcane bagasse ash (SCBA) was scanned at a normal state, while clays (BC and DC) at normal

state and after calcined to 600 °C for 2 hr. Samples for the X-ray analysis were prepared by placing 0.2-0.4 g of the powder sample in an aluminum holder. The sample holder surface was smoothed off to absorb the X-ray beam regularly. The diffraction pattern is plotted within the XRD machine by generating a scan with continuous scanning mode for peak intensity as the Y-axis versus (2θ) as the X-axis. And the diffraction data pattern of samples was analyzed by search match against the international center for diffraction data (ICDD) database using the software expert high score (Iqbal, 2008).

3.3.4 The Plasticity of Clays

The plasticity parameter of Atterberg limits (liquid limit (LL), plastic limit (PL), and plastic index (PI)) was measured by using the Casagrande method following ASTM D4318 (ASTM D4318 et al., 2005).

Liquid limit values were determined for a portion of soil finer than the No.40 sieve. 200 gm of soil was prepared and mixed thoroughly with distilled water into a uniform paste. A portion of the paste was placed in the Casagrande cup and leveled. A groove was cut at the center of the clay paste using the standard grooving tool. Four test trials had been carried out for each proportion of both clays by adjusting the water contents so that the number of blows required to close the groove fall within the range of 15 to 35 blows. The water content of the clay taken near the closed groove was found out the water content of the soil and the cup was altered. The test trials were repeated. A plot of water content against the log of blows was made, and the water content at 25 numbers of blows was determined as the liquid limit. On the other hand, the plastic limit was determined by taking 15 gm of soil passing through a sieve. No. 40 was mixed thoroughly with water. The soil was rolled on a flat glass plate with hand until it becomes 3-4 mm in diameter. This procedure of mixing and rolling was repeated until the soil shows signs of crumbling and the diameter becomes 3 mm. The moisture content at which the threads of clays started to crumble, at the specific diameter, was recorded as the plastic limit (PL) of that clay sample. Finally, the Plasticity indices of clay will be calculated by subtracting the result of the plastic limit from the liquid limit

$$PI = LL - PL \quad \text{.....(3.1)}$$

3.3.5 Particle Size Distribution of Clays

The particle size distribution of clays finer than 75μm can be done by hydrometer test and courser than 75μm by sieving (wet sieve analysis) following ASTM D422-63 test method (ASTM D422, 2007).

The wet sieve analysis was carried out by sieving a 1000 gram weight of air-dried soil sample through the set of sieves placed one below the other after washing by water. The washed air-dried soil sample retained on a 75μm sieve was dried in an oven for 24 hours at 110 °C. After dried, the sample was sieved so that the openings decrease in size from the top sieve down, with a pan at the bottom of the stock after oven-dried of the sample. The whole set of sieves were given a horizontal shaking for about ten minutes until the weight of soil remaining on each sieve reaches a constant value. The hydrometer test method was conducted for soil particle size smaller than 75μm (passing 200 mesh sieves). In general, it was conducted to know the silt and clay fractions based on the ASTM test standard (ASTM D422, 2007). A 50 gm of soil passing sieve No. 200 were agitated with water and dispersing agent (Sodium hexametaphosphate) in a 1000 ml jar. Readings were taken at intervals of 0.75, 1, 2, 4, 8, 15, 60, 120, 240, and 1440 minutes with the hydrometer remaining in the suspension. The corresponding temperature of the suspension was also recorded with a thermometer. After the twenty-four-hour reading, all the reading data were compiled and determined for different sieve sizes for the different hydrometer reading values. Then, the combined grain size distribution curve for particles wet sieve (retained on No.200 sieve) and hydrometer tests (passing No.200 sieve) was drawn.

3.4 Porcelain Electrical Insulator Bodies Formulations

In view of the fact that the study was based on the investigation for the partial incorporation of SCBA in the porcelain electrical insulator body compositions, the optimized batch composition, which was 50% clay, 40% feldspar, and 10% quartz that was named as SCBA0 on this study, was taken from the previous research on porcelain insulator production in Ethiopia (Merga et al., 2019). Generally, the four porcelain insulator bodies were formulated by keeping clay amount in constant 50wt% and quartz 10%, in all batches and varying the percentage composition of feldspars and SCBA waste to observe the effect of partial substitution of feldspar by SCBA waste on the porcelain insulator as indicated in table 3.1. In this study, mixed feldspar was used because, as

shown from the chemical composition result (table 4.1), the percentage of fluxing oxide, mainly K_2O and Na_2O, used to lower firing temperature was low compared to that reported by (Moyo & Park, 2014). To solve the low amount of alkaline oxide on the individual feldspar, mixed feldspar was used from two deposits: Arereti and Wolkite. In addition to the natural raw material, it was also used the recyclable material (SCBA) to partially replace the natural feldspar to get the optimum alkaline oxide content to lower the firing temperature and save time the excessive natural raw material usage. The other reason to use feldspar was to use feldspar minerals properly from different deposits and, at the same time to study their potential for ceramic product production. The prepared powder mixtures are named SCBA0, SCBA10, SCBA15, and SCBA20, where SCBA stands for sugarcane bagasse ash waste and 0, 10, 15, and 10 denotes the weight percentage of sugarcane bagasse ash (SCBA) in the composition. The SCBA waste was added to kaolin and quartz to replace feldspar partially.

Table 3.2: Batch Composition of Porcelain Insulator samples (wt%)

Raw material (wt.%)	SCBA0	SCBA10	SCBA15	SCBA20
Clay	50	50	50	50
Mixed feldspars (AF and WF in 50:50 ratio)	40	30	25	20
Quartz	10	10	10	10
Sugarcane bagasse ash (SCBA)	0	10	15	20

3.5 Preparation of Porcelain Electrical Insulator

All these materials were blended According to the percentage composition presented in Table 3.1. A total of 132 (108 for physical and electrical strength test and 24 for mechanical strength test) samples were carefully weighed using a digital scale from the four compositions. The weighed samples were charged into a ball mill containing porcelain grinding pebbles of different sizes and weights. The ball mill was powered to constantly roll for six hours for each of the four batch compositions (Table 3.1) before its content was discharged completely to achieve particle homogeneity throughout the body. The milled powder samples were adequately weighed, and 7%

of water was added to make it suitable for dry pressing. A hydraulic jack of 10-ton capacity was used for the dry pressing. This was actualized by measuring each sample into an iron steel mold to shape the pieces into the desired dimension. For this study, a cylindrical shaped 80mm diameter and 5mm thickness were prepared from each batch for physical (water absorbance, bulk density, apparent porosity) and electrical (dielectric strength) properties test. At the same time, a rectangular-shaped test body of 75mm length, 38mm width, and 7mm depth was designed from the selected batch (good electrical properties) for mechanical properties test. The mold was done using a hydraulic press, using a pressure of 20 MPs and approximately 3 minutes loading. After the dry pressing, the samples were allowed to dry at room temperature and later placed in the kiln for firing at three different temperatures, 1200 °C, 1250 °C, and 1300 °C, separately. All batches at each specific firing temperature will have three firing times (1.5hr, 2hr, and 2.5hr) with a heating rate of 10°C /min and 5°C /min cooling rate.

3.6 Characterization of Fired Porcelain Electrical Insulator Samples

3.6.1 Physical Properties Test

3.6.1.1 Water Absorbance, Apparent Porosity, and Bulk Density

Water absorption, apparent porosity, and bulk density of porcelain electrical insulator samples were performed according to ASTM standard C 373-88 (ASTM C373-88, 1999). The dry weight of the porcelain electrical insulator sample was measured and noted. Sometimes test samples break during saturation or boiling, so dry weight can be taken after the process completes. Distilled water was filled in the water bath, and placed the fired porcelain electrical sample carefully inside it. The whole system was kept on the heater for boiling it. The fired piece should be completely immersed in water throughout the boiling period, and further water can be added if the water level goes down. Boiling was done for 4 hours. After boiling, samples were completely immersed in water and kept soaking in the same water for 24 hours. Suspended weight was measured for each sample after the soaking of the sample and noted. Suspended weight was calculated by keeping the sample on a wire loop suspended in water and attached to a balance on the other ends.

Saturated weight (soaked weight) was measured after removing all the visible water droplets present on the sample's surface using a wet cloth. After this sample was weighed using balance

and weight sample noted. Similarly, all-porcelain electrical insulator samples were weighed. Weight measurement should be done immediately to avoid errors.

Apparent porosity = (M – D)/ (M – S)] x 100 .....(3.2)

Bulk density = D/ (M – S).....(3.3)

Water absorption = [(M – D)/D] x 100 ..... (3.4)

Where, M = Soaked weight, S = Suspended weight, D = Dry weight

3.6.2 Electrical Properties Test

3.6.2.1 Dielectric Strength

Dielectric strength for insulator samples was computed by measuring their breakdown Voltage using a high voltage testing machine (model TERCO HV 1103), found at Addis Ababa University, department of electrical engineering. The positive and negative terminals of the instrument were connected at either end of the insulator sample, then the voltage was gradually increased from the control disk until the voltage increment break and began to drop displayed on the control disk, which indicates the breakdown voltage of the Sample (Ezenwabude and madueme, 2015), then the dielectric strength will be calculated as

$$\text{Dielectric strength} = \frac{\text{break down voltage (kV)}}{\text{the thickness of the sample (mm)}} \quad \ldots\ldots (3.5)$$

3.6.3 Mechanical Strength Test

3.6.3.1 Flexural Strength/Modulus of Rupture

According to the Test Method-I Procedure A, samples were tested in the standard ASTM D790M-9. The test was conducted at the Ethiopian conformity assessment enterprise Addis Ababa with a universal testing machine. A rectangular-shaped with dimensions was 75mm length, 38mm width, and 7mm depth for the three-point bending test. The support span and the rate of crosshead motion were 50 mm, and 2.08 mm/min, respectively. The maximum fracture load was noted, and MOR was obtained as follows.

Flexural strength=3FL / 2Wd² .....(3.6)

Where F= maximum load L = sample length, W = sample width, D =depth of sample

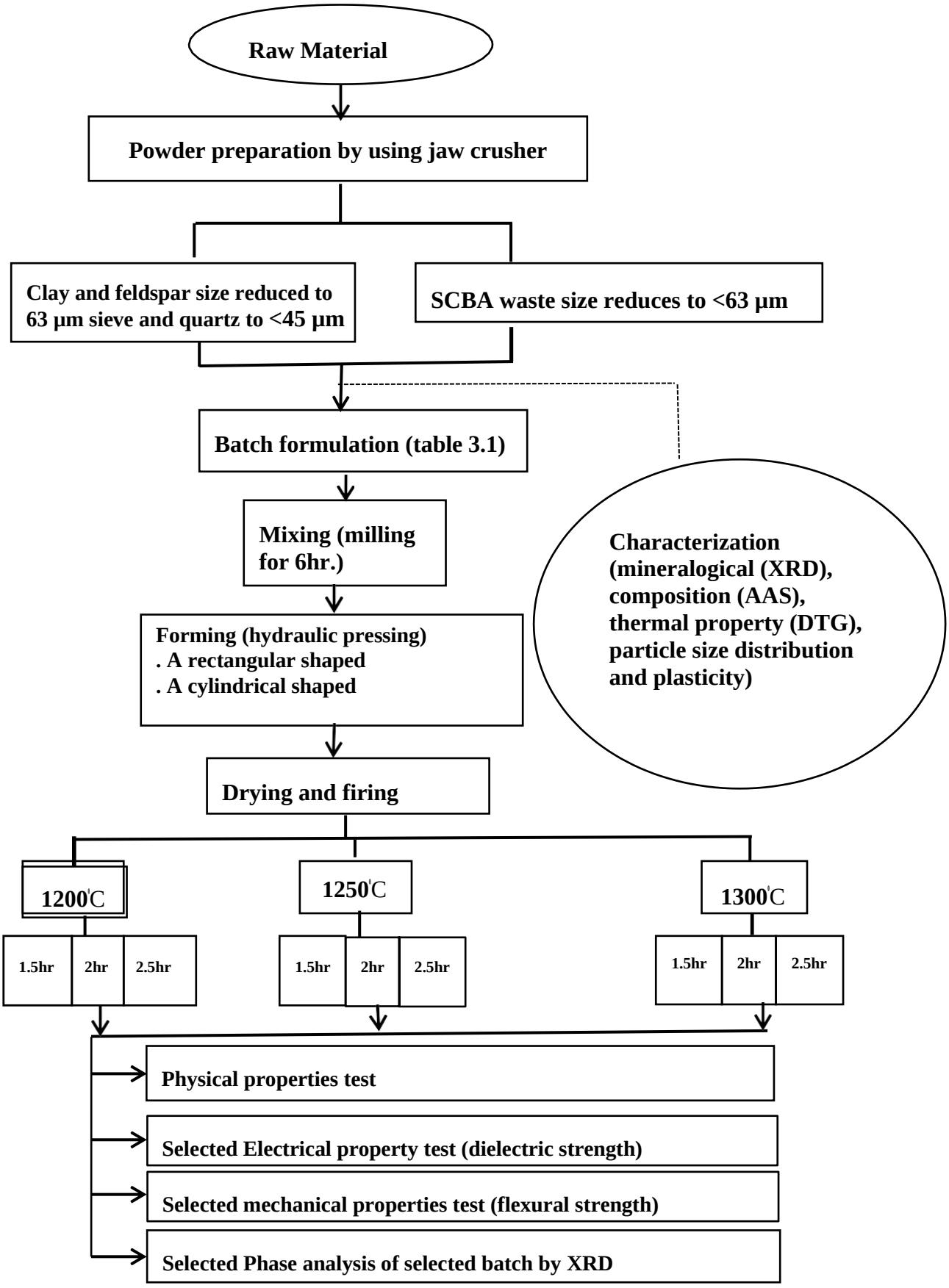

Figure 3.2: Conceptual framework for the preparation of porcelain electrical insulator

4. RESULT AND DISCUSSION

4.1 Characteristics of raw materials

4.1.1 Chemical Composition Analysis

The chemical composition analysis and loss on ignition result of the raw material (clay, feldspar, and quartz) and waste material (SCBA) was given in table 4.1.

Table 4.1: Chemical composition and loss on ignition in (wt %.) of used material.

Oxides	Bombawuha clay (BC)	Denkaka clay (DC)	Arerti feldspar (AF)	Wolkite feldspar (WF)	Chancho Sand (CS)	SCBA
SiO_2	46.72	47.90	72.92	78.12	92.68	65.06
Al_2O_3	35.32	27.84	14.52	13.20	2.94	10.88
Fe_2O_3	0.82	0.32	1.84	1.34	0.48	4.08
CaO	0.74	5.54	0.18	1.32	0.42	1.14
MgO	0.20	0.18	0.20	0.64	0.12	1.30
Na_2O	0.54	Trace	4.66	1.36	Trace	2.06
K_2O	1.08	0.46	1.76	2.26	0.78	6.60
MnO	Trace	Trace	0.06	0.04	<0.01	0.10
P_2O_5	0.07	0.05	0.14	0.08	0.02	0.79
TiO_2	0.03	0.33	Trae	Trace	0.12	0.24
H_2O	0.69	3.50	1.60	1.26	0.44	0.66
LOI	13.85	13.41	1.48	1.63	1.54	4.75

LOI = loss on ignition
trace = quantity detected below 0.1
SCBA = sugarcane bagasse ash

As shown in table 1.1, the chemical composition analysis result of both Bombawuha clay (BC) and Dekaka clay (DC) are characterized by higher silica (46.72 for BC and 47.90 for DC) and relatively lower alumina contents (35.32 for BC and 27.84 for DC). The ratio of the major oxides, SiO_2 to Al_2O_3 of BC, was about 1.3, and DC was about 1.7, which indicated BC much closer to the classical value of pure kaolinite clay. In contrast, DC has a value slightly far from the classical SiO_2/Al_2O_3 ratio of pure kaolinite (1.18) (Mahmoudi et al., 2017). The composition of the

materials concerning other minor oxides, such as the amount of CaO, was very low for BC (0.74), while it was relatively higher in DC (5.54) (Table 1.1). The difference in the amount of CaO suggests that a higher amount of gases may be formed in the firing step and may cause cracks on the fired bodies during calcification and high porosity and water absorption values in the porcelain insulator specimen prepared from DC (Aghayev & Küçükuysal, 2018). Another important aspect concerning the chemical composition of the clay materials is the total amount of alkaline oxides (K_2O and Na_2O) that acting as flux materials, which was higher in BC (1.62%) than DC (0.46%), attributed to the relatively more significant amount of illite and microcline. The LOI value of BC is 13.85% and 13.41% for DC, which was comparable with classical kaolinitic clays (14%) (Tsozué et al., 2017). This confirmed both the clay material used in this study contains kaolinite clay mineral. Generally, based on the chemical composition analysis result, the relative purity of the BC and the low level of calcium oxide and high amount of alkaline oxide present in it make BC is much more suitable for the fabrication of electrical porcelain insulators than DC.

The chemical composition of Chancho sand (CS) reveals that the amount of silica and alumina in the quartz sample was 92.68% and 2.94%, respectively (Table 4.1), which, according to the literature (Kimambo et al., 2014), the silica content was lower than the amount required for quartz to be considered suitable for the production of porcelain body (98.0-99.1% and 0.65-0.8%, respectively). Generally, the amount of silica is higher in sand/quartz because quartz/sand is the mineral that consists of silica in crystal form in high amount than other chemical elements (Anbalagan et al., 2010). Besides, the oxides Fe_2O_3 (0.48%), TiO_2 (0.12%), CaO (0.42%), K_2O (0.78%) and MgO (0.12%), were also present in significant levels.

It is seen from Table 4.1 that the amount of silica in Arerti feldspar (AF) and Wolkite feldspar (WF) sample 72.70% and 78.12%, respectively, were within the range of the amount required for feldspar to be considered suitable for the production of porcelain body (66.3-79.5%) (Kimambo et al., 2014). The chemical composition shows that alumina was present in high amount (14.52%) and (13.20%) followed by the total percentage of Na_2O and K_2O (6.43%) and (3.62%) and then LOI (1.48%) and (1.63%) for AF and WF respectively. They were within the range for feldspar to be used in the porcelain body (Kimambo et al., 2014). The chemical analysis (table 4.1) further shows that the percentage of Fe_2O_3 was high in both of the raw materials, which were 1.84% for AF and 1.34% for WF. The maximum Fe_2O_3 ratio must not be more than 0.3%. The presence of

Fe_2O_3 more than the allowed limits will contribute to unwanted variations of the color towards grey rather than white and causes bloating due to the escape of entrapped gases (William Ochen, , Florence Mutonyi D'ujanga, 2019). Thus, magnetic separation should be carried out to decrease the iron oxide contamination of both feldspar deposits. Moreover, AF shows that sodium feldspar (albite) is the central fluxing oxide because its Na_2O value was 4.66% compared to other flux oxides K_2O and CaO with 0.76 and 0.18%, respectively, while WF related to the type of feldspar anorthoclase, which has a nearly equal amount of K_2O and Na_2O.

According to Table 4.1, from the chemical composition result, the most abundant oxides in sugar cane bagasse ash (SCBA) samples are SiO_2, Al_2O_3, Fe_2O_3, K_2O, and Na_2O. In contrast, CaO, MgO, TiO_2, and P_2O_5 are present only in small quantities. This tendency is very similar to the natural feldspar used in this study, except for the silica, which is present in a lower amount (65%) when compared with natural feldspar (72.70% for AF and 78.12% for WF) and in the iron oxide content, which presents in high amount (4.08%). Moreover, the alkaline oxide (K_2O and Na_2O) content of SCBA (8.66%) was in higher amount as compared to the natural feldspar, which is 6.42% for AF and 3.62% for WF. and this composition provides the SCBA waste properties similar to feldspar (non-plastic material composed mainly of silica sand/quartz and alkaline oxide). Here in this investigation, the partial replacement of feldspar by SCBA waste appeared very comprehensive in the production of porcelain electrical insulators. This is because a higher amount of fluxing oxides (Na_2O, K_2O) in ash composition improved the quality of porcelain electrical insulators by fusing at lower temperatures and dissolving materials like quartz, which melt at higher temperatures in reducing the cost of production and saves the natural raw material. Moreover, from table 4.1, the average loss on ignition (LOI) SCBA waste was 4.75%. This indicates that SCBA has slightly more organic compounds than natural feldspar, and a high LOI value indicates unburned carbon (Agredo et al., 2014).

4.1.2 Mineralogical Analysis

The XRD patterns of Bombawuha clay (BC) and Denkaka clay (DC) are shown in figure 4.1. Results of normal X-ray diffraction analysis of BC and DC samples are given in figure 4.1 (b). XRD result identified the following for the BC; kaolinite (ICDD Card No: 01-080-0885), Illite (ICDD Card No: 00-029-1496), quartz (ICDD Card No: 01-085-0459), Gibbsite (ICDD Card No: 00-029-0041), and microcline (ICDD Card No: 01-083-1604). At the same time, DC consists of

kaolinite (ICDD Card No: 01-083-0971), Quartz (ICDD Card No: 01-085-1054), and nepheline (ICDD Card No: 01-079-0991)

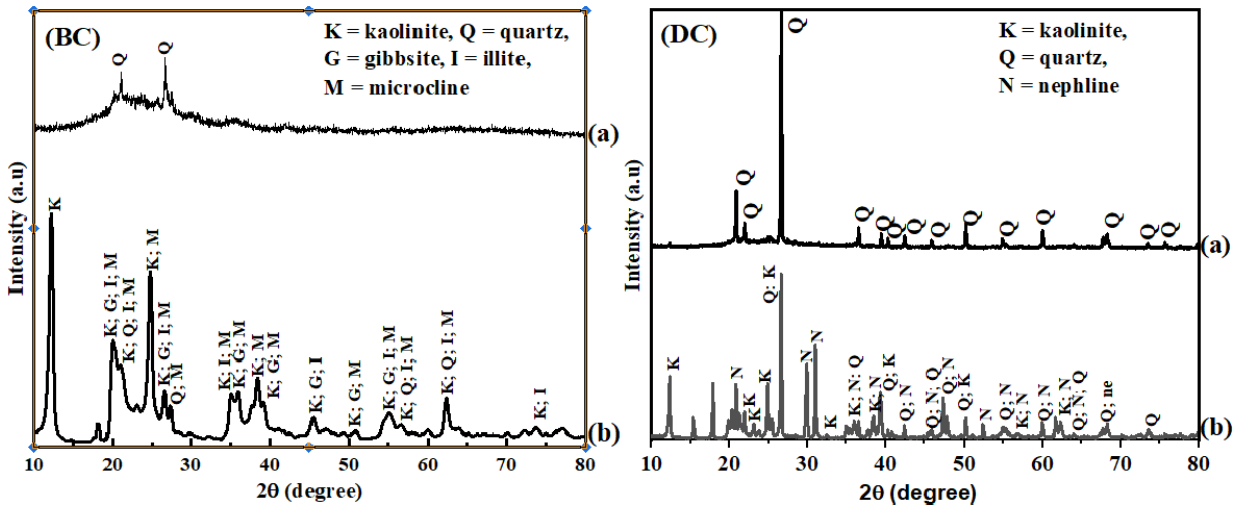

Figure 4.1: XRD partern of BC and DC. (a) calcined at 600°C, (b) normal clay

As shown in the XRD pattern, the higher intensity associated with kaolinite minerals for BC shows the dominance of kaolinite type minerals over other non-clay minerals such as quartz, feldspar, and gibbsite. At the same time, DC characterized the dominance of quartz and kaolinite. Generally, DC has relatively more quartz and minor clay mineral than BC, resulting in a higher SiO_2/Al_2O_3 ratio for DC (1.72) than for BC (1.32), as shown in the chemical analysis data in table 1.1. This shows the crystalline phases identified are in agreement with the results observed by AAS (table 4.1)

After heat treatment, the XRD patterns exhibit a significant change in comparison with the pattern of untreated kaolin (Figure 4.1b), characterized by the disappearance of the diffraction peaks of kaolin, accompanied by the appearance of amorphous aluminosilicate. The XRD peaks narrowed due to the loss of hydroxide structure during the heat treatment process, which is the characteristic X-ray diffraction pattern of metakaolin. These reflections confirm the presence of the kaolinite phase, which transformed to metakaolinite above 450 °C. The presence of intense diffraction peaks is due to the quartz, which remained intact upon the calcination temperatures in this work (Ayele, 2016). Therefore, metakaolin can describe as an amorphous material containing free silica, free alumina, as reported by Brindley (Brindley & Nakahira, 2006).

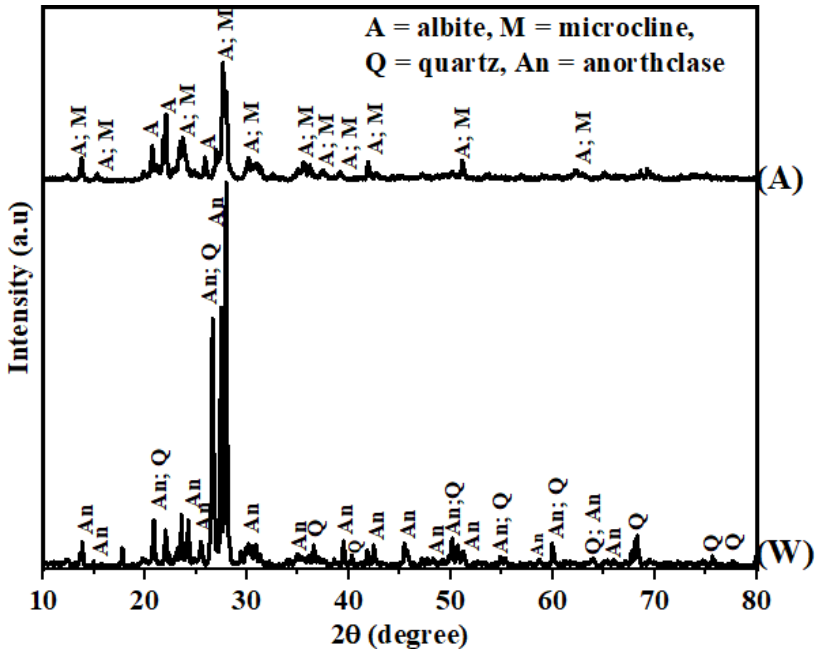

Figure 4.2: XRD pattern of (A) AF and (W) WF

XRD patterns of the investigated feldspar minerals are shown in figure 4.2. The patterns, upon identification and matching of the peaks with ICDD data, reveal that the Arerti feldspar (AF) contains primarily albite (ICDD Card No: 00-083-1610) and microcline (ICDD Card No: 00-087-1789). In comparison, the Wolkite feldspar (WF) is predominantly composed of anorthoclase (ICDD Card No: 01-084-1455) and quartz (ICDD Card No: 01-078-1252). The presence of Albite in AF is due to the higher amount of Na_2O in Arerti feldspar than the Wolkite feldspar, as evidenced by the chemical analysis in table 4.1.

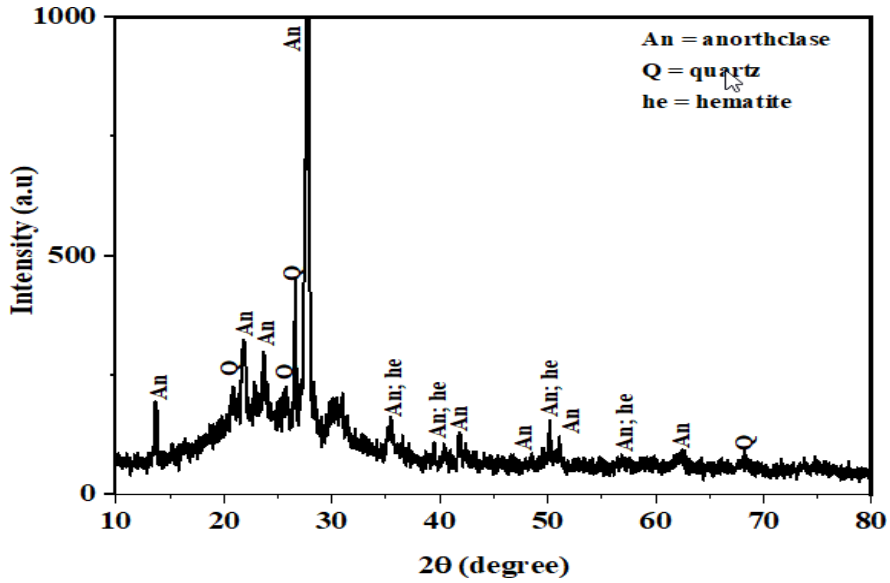

Figure 4.3: XRD pattern of sugarcane bagasse ash waste (SCBA)

Results of X-ray diffraction analysis of sugarcane bagasse ash (SCBA) samples are given in figure 4.3. The XRD result revealed that anorthoclase (ICDD Card No: 01-075-1632) is the primary mineral, followed by hematite (ICDD Card No: 01-073-0603) and then quartz (ICDD Card No: 01-085-0797). This mineralogy gives the ash properties similar to feldspar, used by the porcelain insulator industry to decrease the firing temperature.

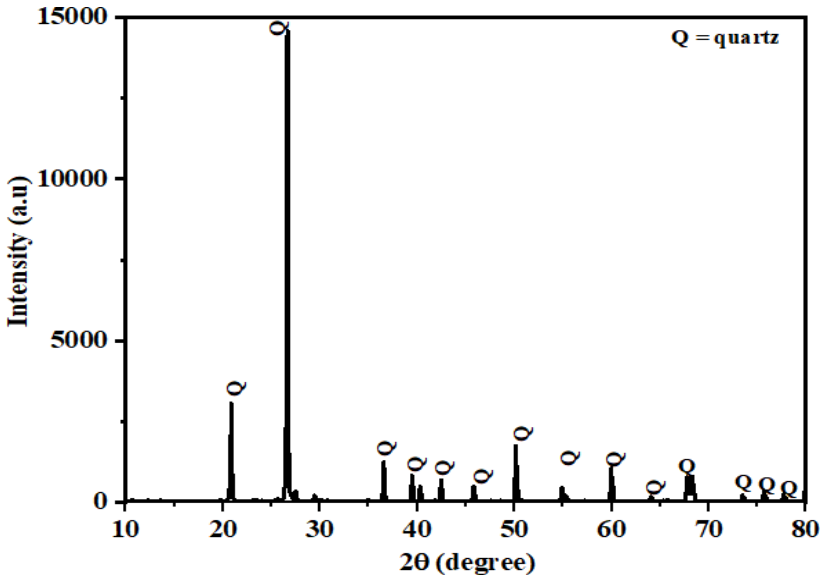

Figure 4.4: XRD pattern of chancho sand (CS)

The XRD patterns of Chancho sand (CS) sample presented in figure 4.4. As can be seen from this figure, this sand is characterized by predominantly contain the reflection of pure quartz minerals as compared to ICDD PDF No (00-083-2465).

4.1.3 Thermal Analysis

The thermal analysis of Bombawuha clay (BC) and Dankaka clay (DC) was measured using the DTA-TGA device, and the results are shown in figure 4.5. The TGA-DTA results were plotted together to correlate the thermal behavior of the clays during firing. A significant endothermic peak at 65.67 ºC for BC and 53.93 ºC for DC can be attributed to removing adsorbed and interlayer water of clay minerals such as kaolinite platelets. The clay materials exhibit an endothermic reaction related to the desorption of surface water (e.g., H_2O on particle surfaces) at low temperatures (<100 ºC) (Holanda, 2012). The mass loss associated with this peak is about 1% for both clays. Besides, a weak endothermic valley was observed at 260.38 ºC for BC; this could be related to the evolution of water vapor resulting from dehydration or hydroxides such as Gibbsite. This is consistent with the results of XRD (figure 4.1). The Gibbsite loses hydroxyl groups to form a transition alumina phase (Mercury et al., 2011). The small endothermic peak at 748.11 ºC for the DC can be attributed to the decomposition of calcite into calcium oxide coherent with the AAS result (Çelik, 2017). The weight loss associated with this was 5.5%. A broad endothermic band centered at 512.02 ºC for BC and 554.71 ºC for DC is due to the dehydroxylation of kaolinite during the phase transformation to metakaolinite and α→β-quartz transformation. The temperature between 420 ºC and 660 ºC is the characteristic range for metakaolin phase formation from kaolinite-type clay minerals (Iqbal, 2008; Yaya et al., 2017). This kaolinite formation can be recognized by removing structural hydroxide in water from the octahedral coordinate of aluminum sheet in kaolinite minerals. Moreover, the phase transformations of kaolinite to metakaolinite were confirmed by the XRD patterns (figure 4.1 (a)), which is calcined at 600 ºC for 2hr indicates 600 ºC is the temperature at which complete formation of metakaolinite is observed. The BC (about 9.84%) undergoes the mass loss associated with this endothermic peak (about 7.75% for the DC). The temperature range of kaolinite to metakaolinite phase transformation is in the range of 420-660,

$Al_2O_3.2SiO_2.2H_2O$ (420-660 ºC) $Al_2O_3.2SiO_2 + 2H_2O$

Kaolinite metakaolinite

The DTA-TGA curve of the sample also shows an exothermic event. A weak exothermic peak at 1006.06 ºC for DC (Fig. a) and a slightly more intense one at 1001.23 ºC for BC sample (Fig. b) was observed due to mullite formation. This exothermic reaction is mainly caused by the recrystallization of new phases from metakaolinite (Celik, 2010).

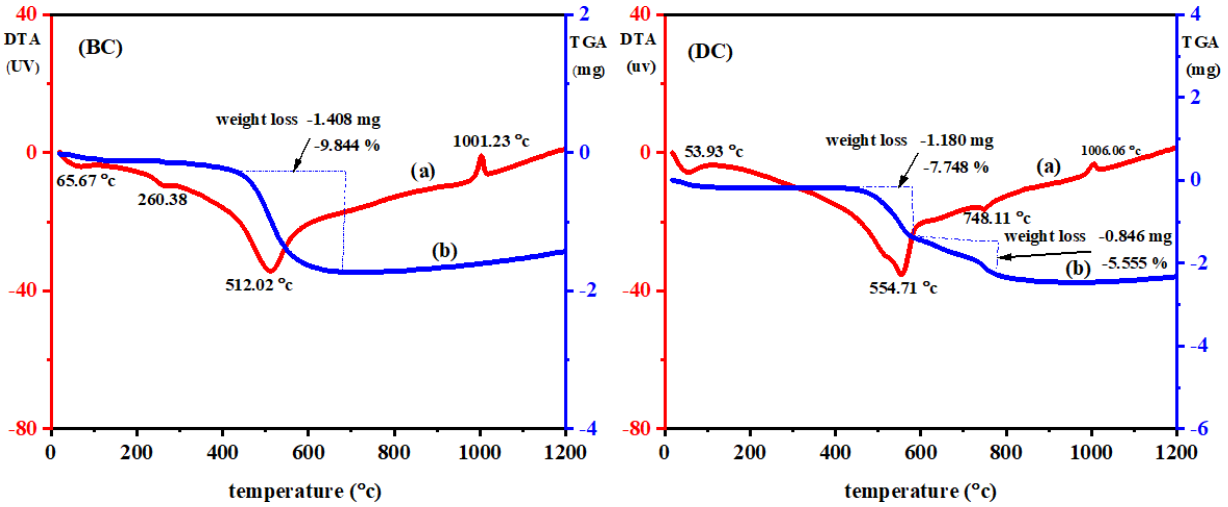

Figure 4.5: Thermograms for BC and DC; (a) DTA (b) TGA

4.1.4 Particle Size Distribution Analysis

The particle size distribution analysis is summarized in table 4.2 and figures 4.6. The result shows that clay minerals (particles with sizes <0.002 mm) were about 20.58% for BC, whereas 12.7% for DC. The silt fraction (particles with sizes between 0.075 and 0.002mm) was approximately 79.11% for BC and 56.03% for DC. The sand fraction (particles with sizes 4.75 – 0.075 mm) was about 0.39% for BC and 31.8% for DC.

Table 4.2: Particle Size Distribution expressed in weight percentage (wt %.) of the two clays.

Particle size distribution	**Sample name**	
	BC (wt %.)	DC (wt %.)
<0.002 mm	20.50	12.17
0.075 – 0.002mm	79.11	56.03
4.75 – 0.075 mm	0.39	31.8

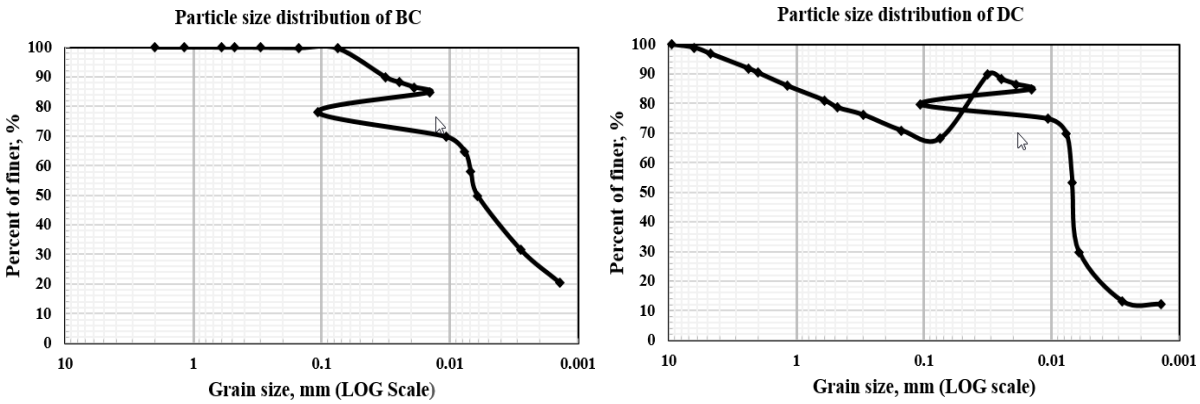

Figure 4.6: Particle Size Distribution of BC and DC

From the particle size distribution result, it was observed that the high silt content in both BC and DC samples indicates that pre-treatment such as crushing and sieving would be necessary before using them for the manufacture of porcelain insulators. In addition, in comparison, BC was characterized by a high amount of clay fraction and a minimal amount of quartz than DC.

4.1.5 Plasticity (Atterberg Limit) Analysis

The plastic limit (PL), liquid limit (LL), and plastic index (PI) values of Bombowha clay (BC) and Denkaka clay (DC) were given in Table 2.

Table 4.3: Liquid limit, plastic limit, and plasticity index of BC and DC samples.

Atterberg limit tests (wt %.)	**BC**	**DC**
Liquid limit (LL)	32	21.7
Plastic limit (PL)	20.8	17.5
Plastic index (PI)	11.3	4.2

The plasticity test result from table 4.3 shown that the liquid limit of BC and DC was measured as 32% and 21.7%, respectively, while the plastic limit was found to be 20.8% for BC and 17.5% for DC. Based on the Atterberg limits, the plastic index is calculated as 11.3% for BC and 4.2% for DC. Based on plastic index (PI) results, according to Atterberg classification, BC is characterized with the middle range of plasticity (7 % < PI > 17%), whereas DC exhibits low plasticity (PI<7%) (Roy & Kumar Bhalla, 2017). At the same time, according to the calculated consistency limits plotted on the Holtz & Kovacs (1981) diagram (Figure 4.8), confirms BC accommodates in a medium plastic zone while DC is located in the low plastic region.

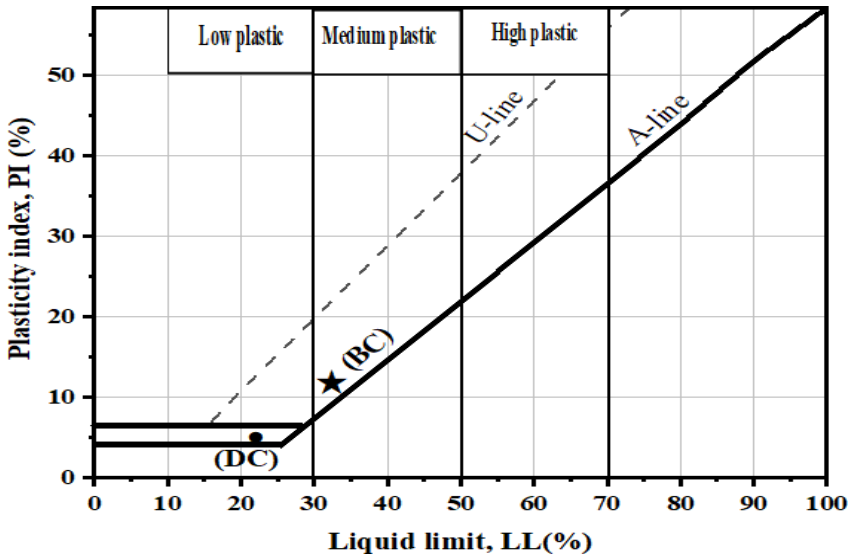

Figure 4.7. Position of BC and DC clay sources on the Holtz and Kovacs plasticity chart.

Among the liquid limit tests, the most important is the plasticity index. Generally, as shown from table 4.3 and figure 4.7, BC has a more plastic index (PI) than DC. This was due to BC having more clay fraction (<2µm) as indicated in the particle size analyses result (table 4.3), the small

amount of non-clay minerals such as quartz, and the presence of interstratified clays like illite, which has more plastic property than kaolin and their presence are shown in the XRD analysis (figure 4.1). On the other hand, the present high amount of quartz and the absence of interstratified and expandable clays tend to lower the plastic index of DC (Bennour et al., 2015). This observation supported by (Skempton, 1984) observed that the plasticity index of soil increases linearly with the percentage of the clay-sized fraction. (Laskar & Pal, 2012) Also, plasticity depends on soil grain size; as the increase of sand content plasticity index of soil decreases, which might reduce intermolecular attraction force. Due to the reduction of attraction force, the liquid limit of the soil decreases, and accordingly plasticity index decreases. But as the clay content increases, the intermolecular attraction force increases, and the liquid limit rises.

4.2 Characterization of Fired Porcelain Insulator

Figure 4.8: Porcelain Bodies after Firing

4.2.1 Phase Analysis

X-ray diffractograms of different porcelain insulator samples as a firing temperature function at a firing time of 2.5hr are illustrated in figure 4.9. The major crystalline phases identified in all compositions were mullite, quartz, and hematite. From the XRD patterns of the composition with control batch (SCBA0) (figure 4.9a) and after the addition of 10% SCBA waste (SCBA10) (figure 4.9b) fired at 1250 °C, it was observed that the peaks associated with the quartz were more intense. When the temperature increased, the intensity of these peaks decreased due to their partial dissolution in the glassy phase (Gralik et al., 2014). Also noted that the peaks relating to the mullite phase become more apparent as the sintering temperature was increased. Figures 4.9c and 4.9d showed the partial replacement of feldspar by bagasse ash in 15% (SCBA15) and 20% (SCBA20), respectively, diffraction peaks of hematite mullite and quartz are present. With the increase in the temperature, the intensity of quartz peaks increased, the mullite peaks decreased, and the hematite peaks nearly remained constant.

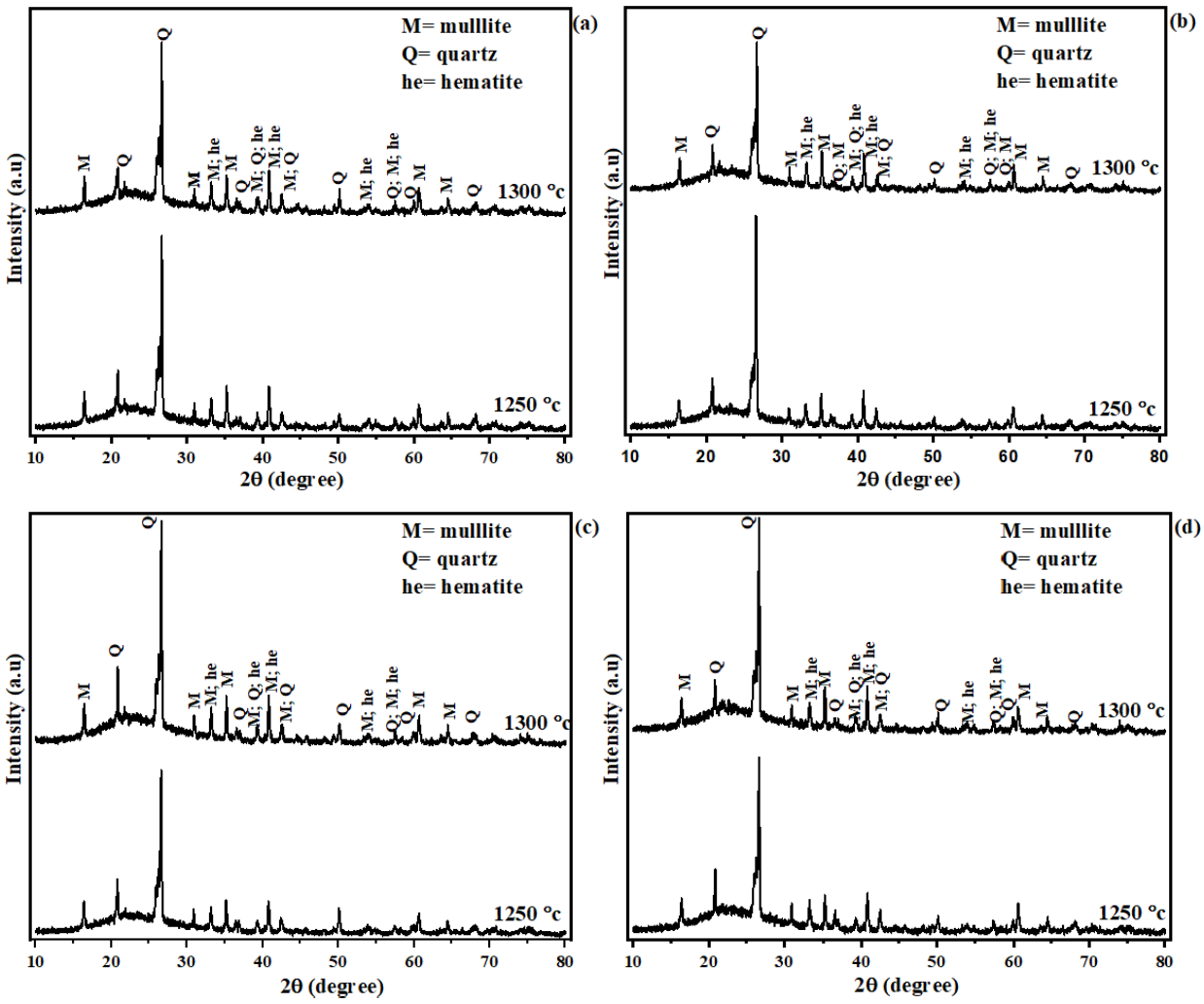

Figure 4.9: XRD patterns of porcelain insulator fired at different temperatures: (a) SCBA0, (b) SCBA10, (c) SCBA15, (d) SCBA20

4.2.2 Physical Property Analysis

The result of the physical properties of porcelain insulator samples at different firing times (1.5, 2, and 2.5hr) and firing temperatures (1200°C, 1250°C, and 1300°C) are shown in table 4.5.

Table 4.4: Physical properties of porcelain insulator at different firing temperatures and firing time

Porcelain insulator sample preparation			Mean of physical properties result		
Batch composition	Firing temperature (°C)	Firing time (hr.)	Water absorption (wt.%)	Bulk density (g/cm^2)	Apparent porosity(wt.%)
SCBA0		1.5	2.24	2.44	5.48
		2	2.16	2.35	5.07
	1200	2.5	1.86	2.39	4.39
		1.5	0.88	2.45	2.15
		2	0.74	2.45	1.82
	1250	2.5	0.6	2.46	1.49
		1.5	0.08	2.49	0.2
		2	0.2	2.43	0.49
	1300	2.5	0.25	2.46	0.61
SCBA10		1.5	1.47	2.39	3.53
		2	1.24	2.34	2.91
	1200	2.5	1.21	2.4	2.91
		1.5	0.67	2.41	1.6
		2	0.59	2.39	1.4
	1250	2.5	0.35	2.42	0.84
		1.5	0.16	2.36	0.38
		2	0.24	2.35	0.56
	1300	2.5	0.33	2.34	0.76

SCBA15		1.5	1.81	2.34	4.22
		2	1.54	2.38	3.67
	1200	2.5	1.45	2.37	3.45
		1.5	0.94	2.37	2.22
		2	0.8	2.36	1.88
	1250	2.5	0.64	2.37	1.58
		1.5	0.87	2.21	1.93
		2	1.01	2.18	2.19
	1300	2.5	2.18	2.19	4.69
SCBA20		1.5	1.91	2.39	4.57
		2	1.51	2.36	3.56
	1200	2.5	1.22	2.35	2.86
		1.5	0.97	2.33	2.28
		2	0.84	2.29	1.93
	1250	2.5	0.72	2.32	1.68
		1.5	1.65	2.13	3.5
		2	1.99	2.14	4.23
	1300	2.5	2.22	2.12	4.78

From table 4.4, it was observed that with the increase of either SCBA content in the mixture or even firing temperature, the values of water absorption and apparent porosity gradually decreased, and bulk density increased as the firing time was increased from 1.5hr to 2hr and 2.5hr. This was observed from the porcelain insulator made from SCBA0 and SCBA10. But for porcelain insulators made from SCBA15 and SCBA20, this happened only up to the firing time of 2hr, then increased the value of water absorption, apparent porosity, and decreased the bulk density.

Moreover, the batch composition, SCBA10 (50% kaolin, 30% mixed feldspar, 10%, and 10% quartz) fired at 1250 °C with firing time 2.5hr was the best with the addition of SCBA waste in the mixture because they had good physical properties value that fulfills the standard requirement porcelain electrical insulators, i.e., water absorption <0.5% and bulk density (1.71-2.1 g/cm^3) (Ngayakamo & Park, 2018). Additionally, in batch composition, SCBA10 at firing temperature 1300 °C also gets a better physical properties value when compared to the value get in firing temperature 1250 °C. But from an economic perspective, it is better to use a lower firing temperature to save energy costs and production costs.

Generally, the porcelain insulator needs to be fired at the firing time and temperature, giving the minimum value of the apparent porosity. This is because the optimum vitrification is achieved when the apparent porosity reaches a minimum value which is usually zero or just close to it (Kimambo et al., 2014). The optimum firing time on this study at which the porcelain insulator was given the minimum value of the apparent porosity was at 2.5hr. Figure 4.11 showed the result of the apparent porosity of the porcelain insulator as a function of different firing temperatures (1200°C, 1250°C, and 1300°C) at a firing time of 2.5hr.

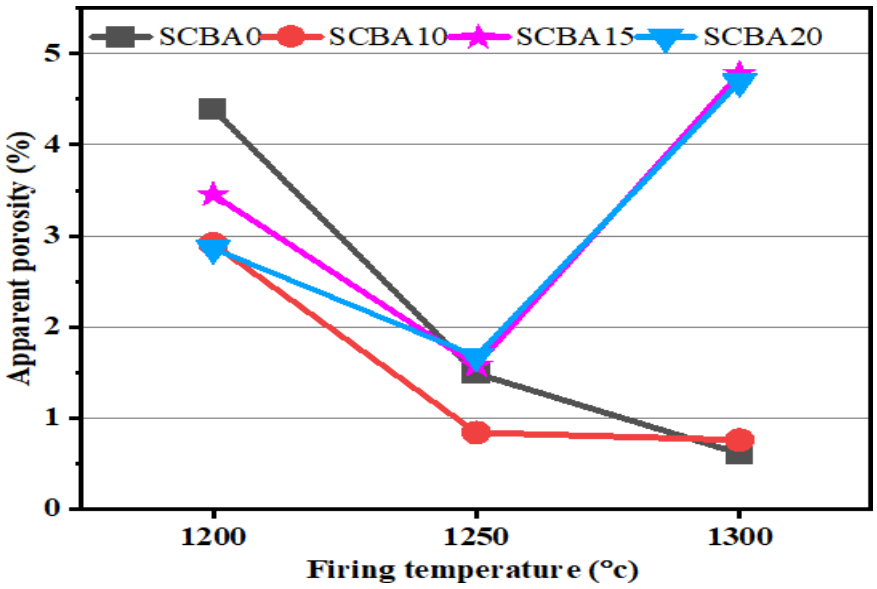

Figure 4.10: Apparent porosity of porcelain samples as a function of firing temperature

The apparent porosity is expected to decrease with an increase in firing temperature. This is because high temperature results in enough liquid phases to block the open porosity (Kimambo et al., 2014). This is expected because as the inter-particle voids/pores are progressively filled up

with increasing sintering temperature, the volume of the ceramic samples can be said to reduce with increased sintering temperature. This behavior is also due to the reduced porosity of the sample, as explained above, which leads to an increase in the amount of matter in the sample per unit volume (Fatai Olufemi, 2015). This took place from the porcelain sample made from composition SCBA0 and SCBA10, where the apparent porosity of the porcelain insulator decreased with an increase in firing temperature.

However, this was not the case for some of the compositions. The apparent porosity for the porcelain insulator made from composition SCBA15 and SCBA20 was found to increase with firing temperature. The increase in apparent porosity at higher firing temperature is thought to be caused by bloating, which takes place as a result of the oxygen released from the reaction of Fe_2O_3 to Fe_3O_4, the expansion of the air enclosed in the pores, and dehydration of OH from the crystal structure of kaolinite started at 500 °C but was trapped in the closed pores (Kitouni & Harabi, 2011). Another possibility to increase apparent porosity may be due to the appearance of a new phase (liquid phase) resulting from fluxing oxide (such as; K_2O and Na_2O) in the raw and waste material used in this work. The appearance of the liquid phase at a higher temperature (1300 °C) allows an easy release of gas trapped in the closed pores, which leads to the formation of new open porosity. The role of the liquid phase in microstructure formation and porosity reduction is not as predominant as in vitrified porcelain (Belhouchet et al., 2019). Furthermore, the porcelain insulator with high content of quartz was expected to have high porosity because as the quartz content increased, the porosity also increased because of the low dry bulk density (Kimambo et al., 2014).

Generally, this work indicated that the apparent porosity depended on the amount of SCBA waste added to the porcelain insulator. The highest porosity of 4.78% was obtained in the fired porcelain insulator containing 20% SCBA (SCBA20) and fired at 1300°C at a firing time of 2.5hr. The lowest porosity of 0.84% at firing temperature of 1250°C for batch composition SCBA10. At the same time, for firing temperature 1300°C, the lowest value was obtained in the porcelain electrical insulator containing 0 and 10% SCBA (as shown in figure 4.10). The porcelain with the lowest apparent porosity has the lowest water absorption, high density, and high flexural strength (Kimambo et al., 2014). This indicated that high SCBA content led to the high porosity of the fired porcelain electrical insulator due to the burning out of SCBA during the firing process. Therefore,

the higher the amount of SCBA in the porcelain insulator, the higher the open porosity and hence the more porous porcelain electrical insulator as a result.

4.2.3 Dielectric Strength Analysis

The values of the dielectric strength of the porcelain insulator sample as a function of firing temperature at 2.5hr firing time are presented in figures 4.11. From figure 4.11, the dielectric strength value was noticed to increase with the addition of sugarcane bagasse ash (SCBA) concentration up to 10 wt.% (SCBA10). It was reduced when the concentration of SCBA increased to 15 (SCBA15) and 20 wt.% (SCBA20) at both firing temperatures (1250 ºC and 1300 ºC). The dielectric strength values obtained for the samples SCBA0 and SCBA10 are within the range of 6.1–13 kV/mm, which is the specified range for porcelain insulators (P. W. Olupot et al., 2010). On the other side, the porcelain insulator samples SCBA15 and SCBA20 yield relatively low dielectric strength, below the standard requirement.

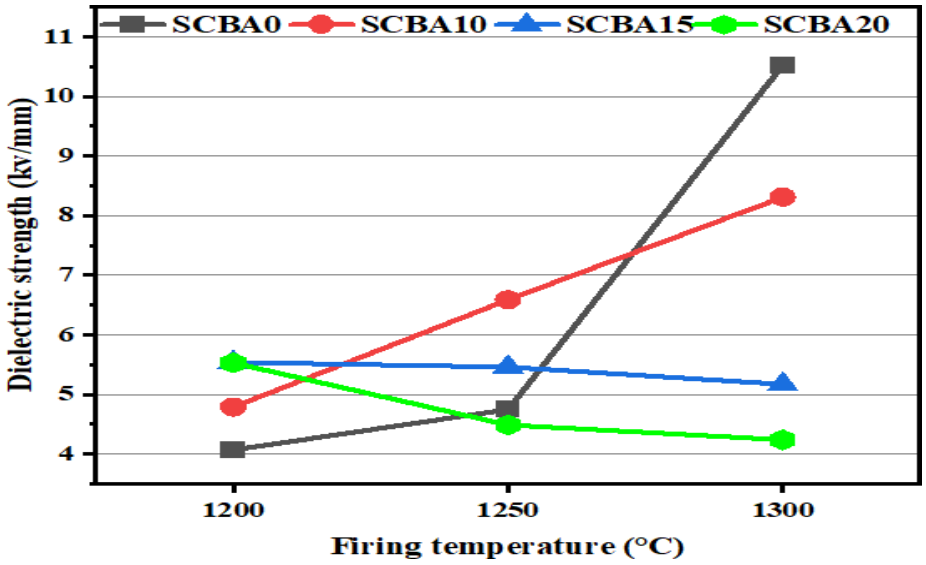

Figure 4.11: The dielectric strength of porcelain insulator as a function of firing temperature

There are various reasons behind increasing and decrease dielectric strength. The porcelain body is composed of phases such as mullite, quartz, and glass. Its electrical properties are dependent on each of these phases (Islam et al., 2004). X-ray diffraction analysis (XRD) showed the presence of mullite, quartz, and a hematite phase in the samples (figure 4.9).

The quartz phase plays a significant role in developing the ultimate properties of the product and appropriate microstructure; only a tiny portion of it gets dissolved in the melt during firing while a considerable amount remains unreacted (Mukhopadhyay et al., 2006). In the unreacted quartz phase during the cooling, there is a significant α-β transformation of quartz at 573 ºC resulting in a 2% decrease in the volume of quartz particles. The resultant volume change may lead to the initiation of the non-coherent interface in structure, microcrack formation, and lowering of electrical properties (De Noni et al., 2009; Moyo & Park, 2014). This is confirmed by the XRD phase analysis shown in figure 4.9, which indicates that when the amount of bagasse ash increased in the mixture, the intensity of the quartz phase increase; this reduced the dielectric strength value. Other authors also supported this observation (Sedghi et al., 2014), who noted that when the silica content decreased, the bending strength increased. At the same time, the dielectric strength of the porcelain also increased to an extent. While (Cajetan et al., 2015) reported that increasing the silica content of their mixture resulted in the increased dielectric strength of the porcelain insulator.

Another phase, which reduces the dielectric strength of porcelain insulators is the presence of a glassy phase. In this study, the glassy phase is derived from the potash feldspar, quartz, and the waste material to partially replace the feldspar (SCBA) component in the porcelain insulator composition. Glass phase has a dominant influence on the electrical and dielectric properties of fired porcelain insulators. The glassy phase will have a harmful effect if the amount is relatively high. When there is a low amount of glassy phase content, it is advantageous to the porcelain insulator. It only fills up the pores and increases the dielectric strength. But when the amount gets higher, it only increases the volume and decreases the density. At the same time, the mobile ions such as Na^{+}, K^{+}, Al^{3+}, and Li^{+} find an easy path to move and hence increase the conductivity (Islam et al., 2004; Kitouni, 2014). That's why it decreases the dielectric strength. Therefore, the porcelain insulator made from the composition SCBA15 and SCBA20, due to having relatively high SCBA waste content, produces a high amount of glassy phase at high firing temperature; thus, its conductivity becomes increased, and their dielectric strength decreased.

In addition to the quartz and glassy phase, hematite also reduces the dielectric properties present in our porcelain insulator samples. According to previous authors (Akwilapo & Wiik, 2003; P. Olupot, 2006), high iron oxide content causes bloating effect due to the transformation of Fe_2O_3 to Fe_3O_4 that affects the electrical properties of the porcelain insulators by reducing bulk density

and increasing the apparent porosity. (Piva et al., 2013) also reported, when hematite was present in amounts (1–3wt %), dielectric properties showed a minimum. Above 3wt% concentration of Fe_2O_3, there was an increase in the dielectric strength.

On the other hand, mullite, a crystalline phase, has a vital role in electrical strength. As the matrix of the ceramic sample is either a clay matrix or the glassy phase, the needle shape mullite maintains the stress level in a higher order than just in a composite matrix (Kitouni, 2014). The formation of mullite from the clay matrix will increase volume by 10%. The increase in volume could heal up cavity or porosity or crack formed due to shrinkage or other reasons (Meng et al., 2012). So, the relatively lower mullite formation in SCBA15 and SCBA20 porcelain insulator samples resulted in a low value of dielectric strength. But for SCBA0 and SCBA10, the high amount of mullite content present, the dielectric strength value was relatively high. In addition, mullite behaves like a semiconductor at high temperatures. The bandgap energy (Eg) of mullite is 1.43 eV, and this value is in the semiconductor interval (Kitouni, 2014).

4.2.4 Flexural Strength (modulus of rupture) Analysis

The combined effect of flexural strength with an increase in firing temperature at a firing time of 2.5hr is shown in figure 4.12.

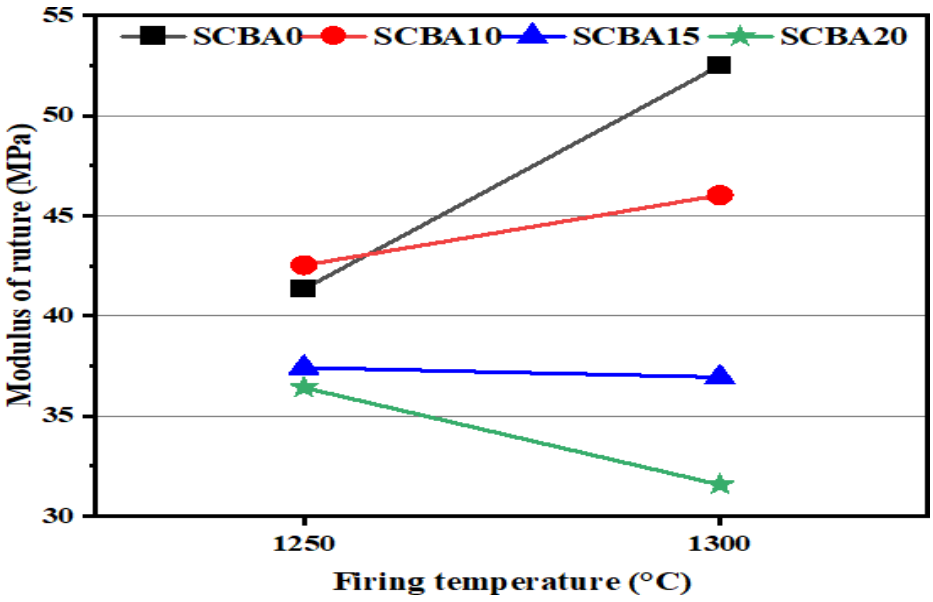

Figure 4.12: The modulus of rupture as a function of firing temperature at firing time 2.5hr.

As observed from the above figure, porcelain insulators' flexural strength increased with increasing firing temperature. This was followed only in compositions SCBA0 and SCBA10, but for composition SCBA15 and SCBA20, the flexural strength of the porcelain insulator was found to decrease with the increase in firing temperature. The increase in flexural strength of the porcelain insulator sample was related to the thermal reactions that were taken place between the constituents of the ceramic batch and those of glass during firing. As the firing temperature increases, the SCBA particles tend to melt, gradually forming what is known as the liquid or glassy phase, which helps cement all the surrounding constituents together. This is often accompanied by a decrease in the pore structure of the fired samples, and as a result, their bulk densities increased. This reflected positively on the flexural strength, i.e., the modulus of rupture strength increases (Darweesh, 2019).

The decrease of flexural strength, in this case, is mainly attributed to that at high firing temperatures, the amount of the liquid or glassy phase is so higher that it migrates up to the outer surfaces of the fired units causing surface bloating, which caused the increase in porosity, and the decrease in both bulk density and flexural strength. On this basis, the higher amount of waste (SCBA) content in the porcelain insulator batch is undesirable, especially with higher firing temperatures (Darweesh, 2019; Kimambo et al., 2014). Moreover, like other properties, this property of the porcelain insulator is also related to the amount of each phase produced. On this basis, the flexural strength of the porcelain insulator was increased as the amount of mullite phase increased. In contrast, it decreased as the content of quartz and hematite increased. It is concluded that the addition of 10% of SCBA waste (SCBA10) and fired at 1250 °C had adequate highest strength of 42.53 MPa as required by ISO 13006 standard requirement (>35 MPa). All the porcelain insulator samples fired at 1250 °C and 1300 °C also fulfill the flexural strength standard requirement for porcelain insulators (>35 Mpa) (Ngayakamo & Park, 2018).

5. CONCLUSION and RECOMMENDATION

This study confirmed for the first time in Ethiopia that the potential of sugarcane bagasse ash (SCBA) to be used as alternative materials for the partial substitution of feldspar for the production of porcelain electrical insulators. This would promote appropriate utilization of the waste instead of discarding it to the environment, which causes adverse effects on human beings and environments.

The SCBA is chemically rich in silica particles (65.06%) and alumina (10.88%). It also contains fluxing compounds like Na_2O, K_2O, etc., which contributed to lowering the sintering temperature up to 50°C during the production of porcelain electrical insulators. However, the high content of Fe_2O_3 in SCBA requires careful sintering of the ceramic raw materials and porcelain samples to avoid the decrease of dielectric strength due to a change in glassy phase structure at high firing temperature.

The chemical composition of raw materials results confirmed that both Bombawuha clay (BC) and Chancho sand/quartz (CS) deposits have suitable porcelain electrical insulator production properties. Bombawuha clay (BC) deposits contain kaolinite clay minerals, low iron oxide content, low calcium oxide content, and good molding workability. Quartz also contains almost pure crystalline silica (92.68wt %) and low iron oxide content (< 0.48 wt %), which is an advantage for porcelain insulator production. The Arererti (AF) and Wolkite feldspar (WF) sources individually contain low flexing oxide content that revealed the mixture of two was better used to get a sufficient amount of flexing oxide.

Moreover, in this investigation, the batch composition SCBA10, which contain sugarcane bagasse ash (10%), clay (50%), feldspar (30%), and quartz (10%) and fired at a temperature of 1250°C and firing time 2.5hr, meet the required standard for porcelain electrical insulators such as having better physical properties (water absorption, apparent porosity, and bulk density), appreciable dielectric strength and mechanical strength that fall within the range, with having optimum mullite and quartz crystalline phase embedded in sufficient glassy phase as characterized by XRD phase analysis. In conclusion, the result confirmed that it is possible to produce high-quality porcelain electrical insulators upon the proper formulation of locally available raw materials (clay, feldspar,

and quartz) and by partial substitution of feldspar with sugarcane bagasse ash for domestic demand in Ethiopia.

Further works

It is recommended to further study for the improvement of fabrication method and the strengthening of porcelains electrical insulator by glazing.

It is recommended that research aimed at optimizing electrical properties (dielectric strength) of porcelain electrical insulators by improving the processing condition through the use of quartz alternatives to overcome crack formation during the firing process.

It is recommended to study the composition SCBA15 and SCBA20 to use for other ceramic ware which doesn't consider the dielectric strength like ceramic wall tiles, etc., because this composition fulfills the requirement of flexural strength (modulus of rupture) (>35MPa) for ceramic wares.

REFERENCES

Abramson, L. W., Lee, T. S., Boyce, G. M., & Sharma, S. S. (1995). Slope stability and stabilization methods. John Wiley and Sons, New York, NY (United States).

Aghayev, T., & Küçükuysal, C. (2018). Ceramic properties of Uşak clay in comparison with Ukrainian clay. Clay Minerals, 53(4), 549–562.

Agredo, J., Mejia, R., Giraldo, C., & González Salcedo, L. (2014). Characterization of sugar cane bagasse ash as supplementary material for Portland cement. Ingenieria e Investigacion, 34, 5–10.

Ajakor, E. M., & Ogwata, C. M. (2015). Indigenous Production of Electrical Porcelain from Nigerian Mineral. International Journal of Scientific and Research Publications, 5(6), 1–4.

Akwilapo, L. D., & Wiik, K. (2003). Ceramic properties of Pugu kaolin clays. Part I: Porosity and modulus of rupture. Bulletin of the Chemical Society of Ethiopia, 17(2), 147–154.

Aliyu, Z. S., Garkida, A. D., Ali, E. A., & Dauda, M. (2016). Characterization of feldspar by instrumental analytical techniques. Characterization of Minerals, Metals, and Materials 2015, 291–297.

Amonette, J. E. (2002). Methods for determination of mineralogy and environmental availability. Soil Mineralogy with Environmental Applications, 7(7), 153–197.

Amonette, J. E., Zelazny, L. W., Karathanasis, A. D., & Harris, W. G. (1994). Quantitative Thermal Analysis of Soil Materials.

Anbalagan, G., Prabakaran, A. R., & Gunasekaran, S. (2010). Spectroscopic characterization of indian standard sand. Journal of Applied Spectroscopy, 77, 86–94. https://doi.org/10.1007/s10812-010-9297-5

Andrade, F. A., Al-Qureshi, H. A., & Hotza, D. (2011). Measuring the plasticity of clays: A review. Applied Clay Science, 51(1–2), 1–7.

Andreev, D. V, & Zakharov, A. I. (2009). Ceramic item deformation during firing: effect of composition and microstructure (review). 50(4), 298–303.

Ash, M., & Chandrasekhar, K. (2017). Enhancing the Performance Consistency of Porcelain Insulators by Understanding Failure Modes: Case Study Approach. IJIREEICE, 5, 1–14.

ASTM C373-88. (1999). Standard Test Method for Water Absorption, Bulk Density, Apparent Porosity, and Apparent Specific Gravity of Fired Whiteware Products. Astm C373-88, 88(Reapproved), 1–2.

ASTM D422. (2007). Standard Test Method for Particle-Size Analysis of Soils. Astm, D422-63(Reapproved), 1–8.

ASTM D4318, ASTM D 4318-10, & D4318-05, A. (2005). Standard Test Methods for Liquid Limit, Plastic Limit, and Plasticity Index of Soils. Report, 04(March 2010), 1–14.

Atkins, P. W. (1996). The elements of physical chemistry. Oxford University Press.

Ayele, L. (2016). Synthesis and Characterization of Zeolite A from Kaolin of Ethiopia: Studies of its application as detergent builder and in tannery wastewater treatment. Unpublished Ph.D thesis submited to Addis Ababa University.

Bader, N. R. (2011). Sample preparation for trace element analysis by Graphite Furnace Atomic Absorption Spectroscopy (GFAAS): An overview. Der Chemica Sinica, 2(5), 211–219.

Baker, D. E., & Suhr, N. H. (2015). Atomic Absorption and Flame Emission Spectrometry. 13–27.

Belhouchet, K., Bayadi, A., Belhouchet, H., & Romero, M. (2019). Improvement of mechanical and dielectric properties of porcelain insulators using economic raw materials. Boletin de La Sociedad Espanola de Ceramica y Vidrio, 58(1), 28–37.

Bennour, A., Mahmoudi, S., Srasra, E., Hatira, N., Boussen, S., Ouaja, M., & Zargouni, F. (2015). Identification and traditional ceramic application of clays from the Chouamekh region in south-eastern Tunisia. Applied Clay Science, 118, 212–220.

Bergmann, C. P. (2004). Traditional and glass powder porcelain : Technical and microstructure analysis. 24, 2383–2388.

Bish, D., & Duffy, C. J. (1990). Thermogravimetric analysis of minerals. Thermal Analysis in Clay Science, 3, 96–157.

Boggs, S. (1995). Principles of sedimentology and stratigraphy. Prentice Hall.

Boussouf, L., Zehani, F., Khenioui, Y., Boutaoui, N., Boussouf, L., Zehani, F., Khenioui, Y., & Boutaoui, N. (2018). Transactions of the Indian Ceramic Society Effect of Amount and Size of Quartz on Mechanical and Dielectric Properties of Electrical Porcelain Effect of Amount and Size of Quartz on Mechanical and Dielectric Properties of Electrical Porcelain. 5456.

Brindley, G., & Nakahira, M. (2006). The Kaolinite-Mullite Reaction Series: II, Metakaolin. Journal of the American Ceramic Society, 42, 314–318.

Cajetan, O. C., O.A., E., C.O., O., C.E., E., & Chike, U. (2015). Characterization of Electrical Porcelain Insulators From Local Clays. International Journal of Research - GRANTHAALAYAH, 3(1), 26–36.

Carty, W., & Senapati, U. (2005). Porcelain—Raw Materials, Processing, Phase Evolution, and Mechanical Behavior. Journal of the American Ceramic Society, 81, 3–20.

Celik, H. (2010). Technological characterization and industrial application of two Turkish clays for the ceramic industry. Applied Clay Science, 50(2), 245–254.

Çelik, H. (2017). Technological characterization and comparison of two ceramic clays used for manufacturing of traditional ceramic products in Turkey. Scientific Mining Journal, 56(4), 137–147.

Cernica, J. N. (1995). Geotechnical engineering. Wiley.

Chang, R. (2005). Chemistry. Chang. McGraw-Hill.

Cherney, E. A., Baker, A. C., Kuffel, J., Lodi, Z., Phillips, A., Powell, D. G., & Stewart, G. A. (2014). Evaluation of and replacement strategies for aged high voltage porcelain suspension-type Insulators. IEEE Transactions on Power Delivery, 29(1), 275–282.

Dana, K., & Das, S. K. (2003). High strength ceramic floor tile compositions containing Indian metallurgical slags. Journal of Materials Science Letters, 22(5), 387–389.

Dana, Kausik, & Das, S. K. (2004a). Evolution of microstructure in flyash-containing porcelain body on heating at different temperatures. Bulletin of Materials Science, 27(2), 183–188.

Dana, Kausik, & Das, S. K. (2004b). Partial substitution of feldspar by B.F. slag in triaxial porcelain: Phase and microstructural evolution. Journal of the European Ceramic Society, 24(15–16), 3833–3839.

Darweesh, H. H. M. (2019). Recycling of glass waste in ceramics — part I: physical , mechanical and thermal properties. SN Applied Sciences, 1(10), 1–11.

Das, B. M. (2008). Advanced soil mechanics. Taylor & Francis.

De Noni, A., Hotza, D., Soler, V. C., & Vilches, E. S. (2009). Effect of quartz particle size on the mechanical behaviour of porcelain tile subjected to different cooling rates. Journal of the European Ceramic Society, 29(6), 1039–1046.

Deer, W. A., Howie, R. A., & Zussman, J. (2001). Rock forming minerals. 1A, 1A,. Geological Society.

Demchuk, V. A., Shchekina, G. B., Kostyukov, N. S., Lukichev, A. A., & Kalinichenko, B. B. (2009). Fabrication of electroporcelain on the Bbasis of raw materials from the Amur rigion. 66, 63–65.

El-Maarry, M. R., Pommerol, A., & Thomas, N. (2013). Analysis of polygonal cracking patterns in chloride-bearing terrains on Mars: Indicators of ancient playa settings. Journal of Geophysical Research E: Planets, 118(11), 2263–2278.

Ergul, S., Sappa, G., Magaldi, D., Pisciella, P., & Pelino, M. (2011). Microstructural and phase transformations during sintering of a phillipsite rich zeolitic tuff. 37, 1843–1850.

Ezenwabude, E., & Madueme, T. (2015). Evaluation of Mixed Local Materials for Low Voltage Insulators. International Journal of Multidisciplinary Sciences and Engineering, 6, 28–38.

Fatai Olufemi. (2015). Effects of sintering temperature on the phase developments and mechanical properties ifon clay. Leonardo Journal of Sciences 2015;26:67-82. Leonardo Journal of Sciences, 26, 67–82.

Fentaw, H. M., & Mengistu, T. (1998). Comparison of Kombelcha and Bombowha kaolins of Ethiopia. 149–164.

Gao, S., Liu, Y., Zhu, M. X., Tao, F. B., Zhou, Z. C., Bo, B., & Huang, Y. J. (2015). Study on

operating properties of ceramic long rod insulator for transmission line. Materials Research Innovations, 19(January), S570–S575.

Gralik, G., Chinelatto, A. L., & Chinelatto, A. S. A. (2014). Effect of different sources of alumina on the microstructure and mechanical properties of the triaxial porcelain. Ceramica, 60(356), 471–481.

Guggenheim, S., Martin, R. T., Alietti, A., Drits, V. A., Formoso, M. L. L., Galán, E., Köster, H. M., Morgan, D. J., Paquet, H., Watanabe, T., Bain, D. C., Ferrell, R. E., Bish, D. L., Fanning, D. S., Guggenheim, S., Kodama, H., & Wicks, F. J. (1995). Definition of clay and clay mineral: Joint report of the AIPEA nomenclature and CMS nomenclature committees. Clays and Clay Minerals, 43(2), 255–256.

Hariharan, V., Shanmugam, M., Amutha, K., & Sivakumar, G. (2018). Preparation and Characterization of Ceramic Products Using Sugarcane Bagasse ash Waste Preparation and Characterization of Ceramic Products Using Sugarcane Bagasse ash Waste. December.

Heaney, P. J., & Veblen, D. R. (1991). Observations of the α-β phase transition in quartz: a review of imaging and diffraction studies and some new results. American Mineralogist, 76(5–6), 1018–1032.

Holanda, K. C. P. F. J. N. F. (2012). Thermal study of clay ceramic pastes containing sugarcane bagasse ash waste. 1–6.

Holtz, R. D., Kovacs, W. D., & Sheahan, T. C. (2013). An introduction to geotechnical engineering. Dorling Kindersley India Pvt. Ltd.

Hossain, S. K. S., Mathur, L., Roy, P. K., Hossain, S. K. S., Mathur, L., & Rice, P. K. R. (2018). Rice husk / rice husk ash as an alternative source of silica in ceramics : A review. Journal of Asian Ceramic Societies, 6(4), 299–313.

Iqbal, Y. (2008). On the Glassy Phase in Tri-Axial Porcelain Bodies. J Pak Mater Soc, 2(2), 62–71.

Iqbal, Y., & Lee, W. E. (2000). Microstructural evolution in triaxial porcelain. Journal of the American Ceramic Society, 83(12), 3121–3127.

Islam, R. A., Chan, Y. C., & Islam, M. F. (2004). Structure-property relationship in high-tension ceramic insulator fired at high temperature. Materials Science and Engineering B: Solid-State Materials for Advanced Technology, 106(2), 132–140.

Jamo, H. U. (2015). Mechanical properties of ceramics tiles by replacement of quartz by RHA and POFA. Unpublished Ph.D thesis submited to Universtiy Tun Hussein Onn Malaysia.

Junkes, J. A., Prates, P. B., Hotza, D., & Segadães, A. M. (2012). Combining mineral and clay-based wastes to produce porcelain-like ceramics: An exploratory study. Applied Clay Science, 69, 50–57.

Kimambo, V., Yoeza, J., Philip, N., & Lugwisha, E. H. (2014). Suitability of Tanzanian kaolin , quartz and feldspar as raw materials for the production of porcelain tiles. 2(6), 201–209.

Kitouni, S. (2014). Dielectric Properties of Triaxial Porcelain Prepared Using Raw Native Materials Without Any Additions. Balkan Journal of Electrical and Computer Engineering, 2(3), 128–131.

Kitouni, S., & Harabi, A. (2011). Sintering and mechanical properties of porcelains prepared from algerian raw materials. Ceramica, 57(344), 453–460.

Kyasager, S. B., & Prasanna, N. D. (2016). Development of Optimum Slip Ratio for High Voltage Porcelain Insulator Manufacturing. International Research Journal of Engineering and Technology, 03(02), 522–527.

Kyonka, J. C., & Cook, R. L. V. (1954). The properties of feldspars and their use in whitewares.

Laskar, A., & Pal, S. K. (2012). Geotechnical characteristics of two different soils and their mixture and relationships between parameters. Electronic Journal of Geotechnical Engineering, 17 U(2004), 2821–2832.

Lawrence, W. (2006). Factors Involved in Plasticity of Kaolin-Water Systems. Journal of the American Ceramic Society, 41, 147–150.

Lawrence, W. G., & West, R. R. (1982). Ceramic science for the potter. Chilton Book Company.

Lee, W. E., & Iqbal, Y. (2001). Influence of mixing on mullite formation in porcelain. 21, 2583–2586.

Looms, J. S. T., & Chapman, M. C. (1991). Insulators for High Voltages. In IEEE Power Engineering Review (Vol. 11, Issue 6).

Mahmoudi, S., Bennour, A., Srasra, E., & Zargouni, F. (2017). Characterization , fi ring behavior and ceramic application of clays from the Gabes region in South Tunisia. 135, 215–225.

Manfredini, T., & Hanuskova, M. (2012). Natural raw materials in “Traditional” ceramic manufacturing. Journal of the University of Chemical Technology and Metallurgy, 47(4), 465–470.

Mark, U., & Onuoha, C. (2018). Characterization of Ibere clay for the prodution of electrical porcelain. February 2019.

Mathur, R., Soni, A., & Kumar, K. (2015). Study on Particle Size Distribution and It ’ s Effects on Shrinkage , Porosity and Bulk Density of Tri-Axial Porcelain Tiles. May, 58–60.

Matteucci, F., Dondi, M., & Guarini, G. (2002). Effect of soda-lime glass on sintering and technological properties of porcelain stoneware tiles. Ceramics International, 28(8), 873–880.

Mejia, E. E. (2013). Characterization of Some Natural and Synthetic Materials With Silicate Structures. Unpublished Ph.D thesis submited to Luleå University of Technology.

Meng, Y., Gong, G., Wu, Z., Yin, Z., Xie, Y., & Liu, S. (2012). Fabrication and microstructure investigation of ultra-high-strength porcelain insulator. 32, 3043–3049.

Mercury, J. M. R., Cabral, A. A., Paiva, A. E. M., Angélica, R. S., Neves, R. F., & Scheller, T. (2011). Thermal behavior and evolution of the mineral phases of Brazilian red mud. Journal of Thermal Analysis and Calorimetry, 104(2), 635–643.

Merga, A., Murthy, H., Amare, E., Ahmed, K., & Bekele, E. (2019). Fabrication of electrical porcelain insulator from ceramic raw materials of Oromia region, Ethiopia. Heliyon, 5.

Mondal, A. H., Bryan, E., Ringler, C., Mekonnen, D., & Rosegrant, M. (2018). Ethiopian energy status and demand scenarios : Prospects to improve energy ef fi ciency and mitigate GHG emissions. Energy, 149, 161–172.

Moraes, J. D. D., Bertolino, S. R. A., Cuffini, S. L., Ducart, D. F., Bretzke, P. E., & Leonardi, G. R. (2017). Clay minerals: Properties and applications to dermocosmetic products and

perspectives of natural raw materials for therapeutic purposes—A review. International Journal of Pharmaceutics, 534(1–2), 213–219.

Mosisa, M., Zereffa, E., Murthy H C, A., & Bekele, E. (2019). Extraction and Characterization of Bio-Silica from Sugar Cane Bagasse Ash of Wonji Sugar Industry, Ethiopia.

Moyo, M. G., & Park, E. (2014). Ceramic Raw Materials in Tanzania – Structure and Properties for Electrical Insulation Application. International Journal of Engineering Research & Technology (IJERT), 3(10), 1015–1020.

Mukhopadhyay, T. K., Ghosh, S., Ghatak, S., & Maiti, H. S. (2006). Effect of pyrophyllite on vitrification and on physical properties of triaxial porcelain. Ceramics International, 32(8), 871–876.

Murray, H. H. (2000). Traditional and new applications for kaolin, smectite, and palygorskite: A general overview. Applied Clay Science, 17(5–6), 207–221.

Murray, H. H. (2007). Applied clay mineralogy: occurrences, processing and application of kaolins, bentonites, palygorskite-sepiolite, and common clays. Elsevier.

Murthy, V. N. . (2005). Geotechnical engineering: Principles and practices of soil mechanics and foundation engineering. New York, N.Y: Marcel Dekker.

Nasejje, S., & Sam, O. (2015). Dependency of Dielectric Strength of Kaolin on Processing Method. Journal of Scientific Research and Reports, 4(4), 306–312.

Ngayakamo, B., & Eugene Park, S. (2019). Evaluation of kalalani vermiculite for production of high strength porcelain insulators. Science of Sintering, 51(2), 1–10.

Ngayakamo, B., & Park, S. E. (2018). Evaluation of Tanzania local ceramic raw materials for high voltage porcelain insulators production. Ceramica, 64, 570–576.

Ngoc, P. Q. (2012). An investigation on petrophysical and geotechnical properties of soils using multivariate statistics An investigation on petrophysical and geotechnical properties of soils using multivariate statistics.

Njoya, D., Tadjuidje, F. S., Ndzana, E. J. A., Pountouonchi, A., Tessier-Doyen, N., & Lecomte-Nana, G. (2017). Effect of flux content and heating rate on the microstructure and

technological properties of Mayouom (Western-Cameroon) kaolinite clay based ceramics. Journal of Asian Ceramic Societies, 5(4), 422–426.

Norton, F. H. (1974). Elements of ceramics. Addison-Wesley Pub. Co.

Ochieng, O. (2016). Characterization and classification of clay minerals for potential applications in Rugi Ward, Kenya. African Journal of Environmental Science and Technology, 10(11), 415–431.

Oladiji, A., Borode, J. O., Adewuyi, B., & Ohijeagbon, I. (2010). Development of Porcelain Insulators from Locally Sourced Materials. Journal of Research Information in Civil Engineering, 7, 47–58.

Olupot, P. (2006). Assessment of Ceramic Raw Materials in Uganda for Electrical Porcelain. Unpublished thesis submited to Universtiy Royal Institute of Technology (KTH).

Olupot, P., Jonsson, S., & Byaruhanga, J. (2014). Development of Electrical Porcelain Insulators from Ceramic Minerals in Uganda. In Ceramic Engineering and Science Proceedings (Vol. 35).

Olupot, P. W., Jonsson, S., & Byaruhanga, J. K. (2010). Development and characterisation of triaxial electrical porcelains from Ugandan ceramic minerals. Ceramics International, 36(4), 1455–1461.

Onwughalu, M. K., & Ogwata, C. M. (2019). Enhancement of Ceramic Insulator Properties with Periwinkle Shell as An Additive. 3(1), 118–121.

Ovri, J. E. O., & Onuoha, C. (2015). Characterization of Some Nigerian Local Clays for Electrical Porcelain Applications. 1(3), 113–119.

Prasad, C. S., Maiti, K. N., & Venugopal, R. (2001). Effect of rice husk ash in whiteware compositions. Ceramics International, 27(6), 629–635.

Prasad, C. S., Maiti, K. N., & Venugopal, R. (2002). Effect of silica fume addition on the properties of whiteware compositions. Ceramics International, 28(1), 9–15.

Rahaman, M. N. (2017). Ceramic processing and sintering (second). Marcel Dekker.

Reeves, G. M., Sims, I., Cripps, J. C., & London., G. S. of. (2006). Clay materials used in construction. The Geological Society.

Roy, S., & Kumar Bhalla, S. (2017). Role of Geotechnical Properties of Soil on Civil Engineering Structures. Resources and Environment, 7(4), 103–109.

Schettino, M. A. S., Siqueira, F. B., & Holanda, J. N. F. (2016). Densification behavior of floor tiles added with sugarcane bagasse ash waste. Ciência & Tecnologia Dos Materiais, 28(1), 60–66.

Silberberg, M. S. (2013). Principles of general chemistry. McGraw-Hill.

Skempton, A. W. (1984). The Colloidal "Activity" of Clays. Selected Papers on Soil Mechanics, 60–64.

Souza, A. E., Teixeira, S. R., Santos, G. T. A., Costa, F. B., & Longo, E. (2011). Reuse of sugarcane bagasse ash (SCBA) to produce ceramic materials. Journal of Environmental Management, 92(10), 2774–2780.

Teixeira, S., da Silva Magalhães, R., Arenales, A., Souza, A., Romero, M., & Rincón, J. (2014). Valorization of sugarcane bagasse ash: Producing glass-ceramic materials. Journal of Environmental Management, 134C, 15–19.

Tonnayopas, D. (2013). Green Building Bricks Made with Clays and Sugar Cane Bagasse Ash.

Tsozué, D., Nzeugang, A. N., Mache, J. R., Loweh, S., & Fagel, N. (2017). Mineralogical, physico-chemical and technological characterization of clays from Maroua (Far-North, Cameroon) for use in ceramic bricks production. Journal of Building Engineering, 11(March), 17–24.

Valásková, M. (2015). Clays, clay minerals and cordierite ceramics - A review. Ceramics Silikaty, 59, 331–340.

Viruthagiri, G., Sathiya Priya, S., Shanmugam, N., Balaji, A., Balamurugan, K., & Gopinathan, E. (2015). Spectroscopic investigation on the production of clay bricks with SCBA waste. Spectrochimica Acta - Part A: Molecular and Biomolecular Spectroscopy, 149, 468–475.

Warshaw, S. I., & Seider, R. (1967). Comparison of Strength of Triaxial Porcelains Containing Alumina and Silica. Journal of the American Ceramic Society, 50(7), 337–343.

William Ochen, , Florence Mutonyi D'ujanga, B. O. (2019). Effect of Quartz Particle Size on Sintering Behavior and Flexural Strength of Porcelain Tiles Made from Raw Materials in Uganda. Advances in Materials, 8(1), 33–40.

Xi, Y., Martens, W., He, H., & Frost, R. (2005). Thermogravimetric Analysis of Organoclays Intercalated with the Surfactant Octadecyltrimethylammonium Bromide. Journal of Thermal Analysis and Calorimetry, 81(1), 91–97.

Xu, Q., Ji, T., Gao, S.-J., Yang, Z., & Wu, N. (2018). Characteristics and Applications of Sugar Cane Bagasse Ash Waste in Cementitious Materials. Materials (Basel, Switzerland), 12(1), 1–19.

Yaya, A., Tiburu, E. K., Vickers, M. E., Efavi, J. K., Onwona-Agyeman, B., & Knowles, K. M. (2017). Characterisation and identification of local kaolin clay from Ghana: A potential material for electroporcelain insulator fabrication. Applied Clay Science, 150, 125–130.

Zbik, M. S., Martens, W. N., Frost, R. L., Song, Y. F., Chen, Y. M., & Chen, J. H. (2010). Smectite flocculation structure modified by Al13 macro-molecules - As revealed by the transmission X-ray microscopy (TXM). Journal of Colloid and Interface Science, 345(1), 34–40.